



Synthesis and characterization of molybdenum trioxide (MoO₃) based nanostructures



by

Jaffer Saddique

(127-FBAS/MSPHY/F12)

Supervisor

Dr. Muhammad Mumtaz

Assistant professor
Department of physics, FBAS,
IIU Islamabad

Co-Supervisor

Dr. Muhammad Sultan

Senior Scientific Officer NS & CD
National Centre for Physics,
Quaid-i-Azam University Islamabad

Department of Physics

Faculty of Basic and Applied Sciences

International Islamic University, Islamabad

(2015)



Accession No TH-14558 (4)

MS
536.5
JAS

- Molybdenum trioxide
- Temperature
- Metal oxides materials.

**Synthesis and characterization of molybdenum trioxide
(MoO₃) based nanostructures**

by

Jaffer Saddique

(127-FBAS/MSPHY/F12)

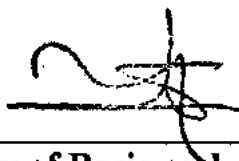
This Thesis submitted to Department of Physics International Islamic University,
Islamabad for the award of degree of MS Physics



Chairman Department of Physics

**CHAIRMAN
DEPT. OF PHYSICS
International Islamic University
Islamabad**

International Islamic University Islamabad



Dean Faculty of Basic and Applied Science

International Islamic University, Islamabad

Final Approval

It is certified that the work presented in this thesis entitled **“Synthesis and characterization of molybdenum trioxide (MoO₃) based nanostructure”** by **Jaffer Saddique**, registration No.127-FBAS/MSPHY/F12 is of sufficient standard in scope and quality for the award of degree of MS Physics from Department of Physics, International Islamic University, Islamabad, Pakistan.

Viva Voce Committee

Chairman _____
(Department of Physics)

Supervisor _____

Co-supervisor _____

External Examiner _____

Internal Examiner _____



DEDICATED

To

My Loving Parents

Brothers

Respected Teachers

And

My Cute

Farhan, and Saad Khattak

Declaration

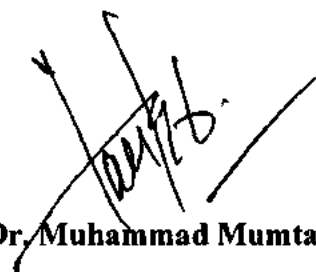
I, **Jaffer Saddique** (Registration # 127-FBAS/MSPHY/F12), student of MS Physics (session 2012-2014), hereby declare that the matter presented in the thesis titled “**Synthesis and characterization of molybdenum trioxide (MoO₃) based nanostructures**” is my own work and has not been published or submitted as research work or thesis in any form in any other university or institute in Pakistan or aboard.

Jaffer Saddique
(127-FBAS/MSPHY/F-12)

Dated: _____

Forwarding Sheet by Research Supervisor

The thesis entitled “**Synthesis and characterization of molybdenum trioxide (MoO₃) based nanostructures**” submitted by **Jaffer Saddique** (Registration # 127-FBAS/MSPHY/F12) in partial fulfillment of MS degree in Physics has been completed under my guidance and supervision. I am satisfied with the quality of his research work and allow him to submit this thesis for further process to graduate with Master of Science degree from Department of Physics, as per IIU Islamabad rules and regulations.



Dr. Muhammad Mumtaz,
Assistant Professor
Department of Physics,
International Islamic university,
Islamabad.

Dated: 28/04/2015

Acknowledgment

My foremost acknowledgement is to that unseen power that governs all the affairs of nature and mans the all mighty Allah, because it was due to the blessing of him that I could complete my research work successfully. At the same time, I offer my humble words of thanks and gratitude to the towering personality of the Holly Prophet (PBUH) fountain of light, guidance and knowledge to all human beings.

I am very thankful to my Supervisor of this project **Dr. Muhammad Mumtaz** and Co-supervisor **Dr. Muhammad Sultan**, who helped me during research work and gave me very useful information's and provided several related research papers about my project. I can never forget his kindness behavior. At the completion of my project; I can never forget the best guidance granted by my best teachers, Dr. Yaqoob Khan.

I am thankful to my friends, Rafi Ullah, Abid Zaman, Abdul Mateen, Imran Ullah khan, Muhammad Mushtaq , Dr. Sleem and Mudassir khattak. I present my special thanks to my sweet friend Mr Hazrat Usman. I am also thankful to Nasir Rehman, who helped me during thesis and Nasir Shaheed (who has made me what I am today.)

Last but not the least , I offer my heartiest words of thanks to my parents, brothers, sister and all of my family members , special thanks to my brother Hamid Ullah Khan ,who encourage me and prayed for me to achieve success in my life

Jaffer Saddique

Table of Contents

CHAPTER 1	1
INTRODUCTION	1
1.1 Introduction to Material	1
1.2 Classification of materials.....	1
1.2.1 Metals.....	1
1.2.2 Ceramics.....	1
1.2.3 Polymers	2
1.3 Semiconductor	2
1.3.1 Intrinsic semiconductor	3
1.3.2 Extrinsic semiconductor.....	3
1.3.2.1 n-type semiconductor.....	3
1.3.2.2 p-type semiconductor.....	4
1.4 Nanotechnology	4
1.4.1 Synthesis approaches of nanotechnology	5
1.4.1.1 Top-down approach	5
1.4.1.2 Bottom-up approach	6
1.4.2 Applications of nanotechnology	6
1.4.3 Classification of nanomaterials.....	7
1.4.3.1 Zero dimensional nanomaterials.....	7
1.4.3.2 One dimensional nanomaterials.....	7
1.4.3.3 Two dimensional nanomaterials.....	8
1.5 Metal oxide.....	8

1.5.1 Metal oxide in nature.....	9
CHAPTER 2	10
Literature Review	10
2.1 Molybdenum trioxide	10
2.1.1 Physical properties of MoO ₃	10
2.1.2 Structure of MoO ₃	11
2.1.3 Optical properties of MoO ₃	12
2.1.4 Nanostructure properties of MoO ₃	12
2.1.5 Application of MoO ₃	13
2.1.6 Molybdenum trioxide used as a catalyst.....	14
2.2 Literature review.....	14
Objectives.....	16
CHAPTER 3	17
Synthesis and Structural characterization	17
3.1 Sol-gel method	17
3.1.1 Steps in sol-gel method.....	18
3.1.2 Applications of sol-gel method	18
3.1.3 Advantages of sol-gel method	18
3.2 Co-precipitation method.....	18
3.2.1 Advantages of co-precipitation method.....	19
3.2.2 Disadvantages of co-precipitation method.....	19
3.3 Sample preparation	19
3.3.1 Chemicals.....	20
3.3.2 Synthesis of h-MoO ₃ nanorods	20
3.4 Characterization techniques.....	22

3.4.1 X-ray diffraction	22
3.4.2 Working principle of X-ray diffractometer	23
3.4.3 Calculation of the average crystallite size	23
3.4.4 Calculation of particle size.....	24
3.5 Scanning electron microscopy (SEM).....	25
3.5.1 Principle of SEM.....	26
3.6 Energy Dispersive spectroscopy (EDX).....	27
3.7 UV/Visible Spectroscopy.....	27
3.7.1 UV/Visible working principle.....	28
CHAPTER 4	30
Result and discussion	30
4.1 Structural phase characterization.....	30
4.1.1 Calculation of average crystallite size of MoO ₃ particles size by using Scherer's formula..	32
4.2 Scanning electron microscopy of pure and chromium doped MoO ₃ at different temperature..	34
4.2.1 SEM of pure h-MoO ₃	34
4.3 Elemental compositional study by (EDS).....	36
4.4 Optical studies by (DRS)	39
Conclusions	44
References.....	45

Table of Figures

Figure 1.1: Schematic diagram of top-down and bottom-up approaches.....	6
Figure 2.1: Structure of MoO ₃	11
Figure 3.1: Flow chart for preparing pure MoO ₃ nano rods.....	21
Figure 3.2: Bragg's reflection from parallel planes.....	22
Figure 3.3: Particles size on diffraction curves.....	24

Figure 3.4: Schematic diagram of SEM	26
Figure 3.5: schematic diagram of UV visible spectrometer.....	28
Figure 4.1: The typical XRD pattern of the pure h-MoO ₃	31
Figure 4.2: XRD pattern of 2% Cr doped MoO ₃	32
Figure 4.3: Combined XRD spectra of doped and pure MoO ₃	33
Figure 4.4: SEM image of pure h-MoO ₃ at low temperature.....	34
Figure 4.5: SEM image of pure h-MoO ₃ at 100 ⁰ C.....	35
Figure 4.6: SEM image of pure h-MoO ₃ at 145 ⁰ C.....	35
Figure 4.7: SEM image of 2wt% Cr doped MoO ₃	36
Figure 4.8: EDS spectrum of pure h-MoO ₃ at 100 ⁰ C.	37
Figure 4.9: EDS spectra of 0.5wt % Chromium doped h-MoO ₃	38
Figure 4.10: EDS spectra of 2wt% Chromium doped h-MoO ₃	38
Figure 4.11: DRS spectra of pure h-MoO ₃	39
Figure 4.12: Combined DRS spectra of doped and pure MoO ₃	40
Figure 4.13: Comparison of K-M doped and pure MoO ₃ samples.....	41
Figure 4.14: Binding energy versus doping concentration graph.....	43

List of tables

Table 2.1: Physical properties of Molybdenum trioxide (MoO ₃).....	11
Table 4.1: Crystallite size of h-MoO ₃	33
Table 4.2: The Quantitative analysis of pure MoO ₃ and Chromium doped MoO ₃ samples.....	39
Table 4.3: Band gap values of doped and pure samples.....	41

Abstract

Low temperature growth technique has been used to synthesize nanostructure metal oxides materials. Hexagonal molybdenum trioxide (h-MoO₃) nanorods doped with chromium were synthesized successfully by using chemical co-precipitation method at low temperature. Reaction conditions were varied to improve the crystallinity of as grown materials as well as to optimize the morphology of the nanorods. X-ray diffraction (XRD) analysis confirmed the hexagonal phase and crystallinity of the as synthesized (h-MoO₃) powder. The average crystallite size of the structure calculated was 38.10 nm. The surface morphology studied was carried out by means of scanning electron microscope (SEM), which showed that the (h-MoO₃) contained one dimensional nano rods with a hexagonal cross section. Energy dispersive spectroscopy (EDX) analysis was used to investigate the compositional analysis of the molybdenum, oxygen and chromium contained by the pure and doped products respectively. UV/visible spectroscopy examined the optical absorption property of (h-MoO₃). The band gap was calculated from Kubelka Munk (K-M) function. The calculated E_g was tuned from 2.99 eV for pure h-MoO₃ to 2.76 eV with 5 wt. % Cr doping.

Chapter No. 1**INTRODUCTION****1.1 Introduction to materials**

The substance by which some what is formed are identified as materials. In our life materials play a vital role, because all the products which we use in our daily life are made of these materials. People use different materials to improve their life style. So advancement in human civilization is directly linked to the use and applications of these materials. Since from last two decades, the main focus is that how to minimize the size of the bulk materials to nano-level. So by varying the size of the material at nano-scale (10^{-9} m) give birth to new properties of the same material known as nano-science. At nano-level the physical and chemical characteristics of material completely changed as compared to that of macro and micro-level [1].

1.2 Classification of materials

Solid materials are classified into three basic categories.

- Metals
- Ceramics
- Polymers

1.2.1 Metals

Metallic materials are usually the combination of metal elements, which consist of large number of free electrons. These free electrons are not confined to any particle atom inside the solid. Many properties of the metal are directly concerned with these electrons. Metals are good conductor of heat and electricity i.e. iron, gold and silver etc [2].

1.2.2 Ceramics

Ceramics are that class of material that lies between metallic and non metallic material. Ceramics are stiff and strong as compared to the metallic elements. Mostly ceramics are composed of Oxides, Nitrides and Carbides. Current and heat cannot passes through ceramics because they have low conductivity [3].

1.2.3 Polymer

Polymer is chemically composed from hydrocarbon and non-metallic elements. Polymer has long chain structure made from carbon and hydrogen i.e. epoxy resin, polyethylene and rubber etc. These materials are practically more elastic having low density. Mechanical properties of the polymers are different from metal and ceramics [4].

In addition to metal, ceramics and polymer, there are three other categories of materials.

- Composites
- Biomaterials
- Semiconductor

1.3 Semiconductor

All those materials which have conductivity in the half way of those conductors and insulator are called Semiconductors. The resistivity of the Semiconductors varies in the range from 10^{-5} to 10^4 Ω -m. Germanium and Silicon are pure semiconductor belongs to group IV of periodic table, having the resistivity of about 0.6 Ω -m and 1.5×10^{-3} Ω -m respectively, are called elementary semiconductor [4]. There is another type of semiconductor which is formed from the combination of group IV and group V elements such as Gallium Arsenide (GaAs), Cadmium Sulphide (CdS) etc, are called compound semiconductors. The band gap of the semiconductor is small as compared to the band gap of insulator. The characteristic band gap of the semiconductor is varies in the range 0.2 to 2.5eV, while that of the insulator is about 6 eV. The importance of the band gap is to measure and determine the wavelength of the radiation which emits or absorbed by the semiconductor [5].

The conductivity of the semiconductor varies with temperature, at 0 K temperatures the pure silicon atom act like an insulator but at high temperature it become a conductor. Therefore, the conductivity of the semiconductor increases with the increasing of temperature. Beside this, the conductivity of the semiconductor can be enhanced by adding some impurity (doping) in semiconductor [2]. Furthermore, semiconductor can be classified into two types.

- Intrinsic semiconductor
- Extrinsic semiconductor

1.3.1 Intrinsic semiconductor

Naturally occurring semiconductors which are free from any other impurities atoms are called intrinsic or pure semiconductor such is pure Germanium or Silicon. In intrinsic semiconductor concentration of electrons in the conduction band are equal to the concentration of holes in valence band [5]. The electrical conductivity of such type of materials can be determined by thermally generated electron inside the crystal. Because the electron in valence band may acquire sufficient energy to break their covalent bond and become free from the atom. These free electrons move randomly inside the crystal referred as a conduction electron. Each electron which break covalent bond in the valence band and go to conduction band, create vacancy left behind in the valence band called “hole” also act as a charge carrier [2].

1.3.2 Extrinsic semiconductor

Semiconductors which are doped with impurity atoms are called extrinsic semiconductor. Impurity atoms are added deliberately to enhance and control the carrier concentration of the semiconductor are called doping. By introducing doping or impurity atoms is the most proficient and suitable method to improve and modify the conductivity of the intrinsic semiconductor [5]. The conductivity of the semiconductor depends on the nature of the doping element. If the impurity atom have one more electron or one less electron that it replace the atom, in this state excess of electron or deficiency of electron are created in it but not present in the host atom. The created free electron or hole inside the material can move freely and conduct electricity. Mostly, elements of group III and group V of the periodic table are commonly use as an impurities atoms to doped with Silicon or Germanium [6].

Therefore by adding some impurities to dope semiconductor with the excess of electron or to donate electron are called n-type semiconductor, and with the fewer of electron or to accept one electron are called p-type semiconductor. The impurities are doped in semiconductor in very small ratio about 1 to 10^6 to 10^8 atoms. Furthermore, extrinsic semiconductor can be classified in two types [2].

- n-type semiconductor
- p- type semiconductor

1.3.2.1 n-type semiconductor

Introducing of group V elements having an atom with five electrons in pure Silicon or in Pure Germanium i.e. phosphorus, Antimony etc, which create an excess of electron in the

crystal are called N-type semiconductor. Four from these electrons make a covalent bond with other nearby four silicon atoms and the remaining fifth electron is loosely bounded to the nucleus. A small and specific amount of energy is needed to take out the fifth electron from atoms and become a free electron inside the crystal to conduct electricity [6].

The energy level which is related to the fifth electron lies nearly beneath to the conduction band edge known is donor level. The energy difference and donor level is nearly about 0.03 eV [5]. Therefore the fifth valence electron is easily relocate to conduction band, left behind a vacancy in the valence band are called hole. Thus each and every pentavalent doping element generate an extra electron and donate this electron to the host material are called donor or n-type semiconductor. In n-type semiconductor materials electrons are in majority are called majority charge carrier while holes are called the minority charge carrier [7].

1.3.2.2 p-type semiconductor

When a group III elements having an atom with three valence electron such is Aluminum, Gallium and Boron etc, are doped with silicon atom which make three covalent bond with nearest three silicon atoms while the fourth one is remain unbounded to the fewer of one electron. So each trivalent impurities atom needs one electron from the nearest neighbor silicon atom to make their uncompleted fourth covalent bond [5]. Very small amount of energy is needed to create one electron. The transferred of electron create a vacancy in the neighbor silicon atom called "hole". The energy level of this electron is just beyond to the valence band .The acceptor level in the case of silicon is about to 0.16 eV. To provide such a small amount of energy an electron can easily transfer from valence band to conduction band. This electron creates a vacancy in valence band in the form of hole which acts as a mobile charge career [6].

The thermally generated electron does not take a part in the conduction of electricity. Therefore, each trivalent impurity atom has a tendency to accept one electron from nearest silicon atom to create a hole in the semiconductor. Such kinds of impurities are known as acceptor or p-type impurities and semiconductors possess such impurities are known as p-type semiconductor. In p-type semiconductor hole are in majority charge carriers and electrons are minority charge carriers [7].

1.4 Nanotechnology

To study the materials at nanoscale, having range from 1 nm to 100 nm and the technology, which deals such type of materials is known as nanotechnology [8].

Nanotechnology get great attention from last two decade due to its wide applications especially in research area of chemistry, physics, material science etc, and also interconnected with other field of science and engineering [9]. Nanotechnology is employed for the synthesis, characterization and fabrication for particularly small nanostructure materials. It gives idea about very small size of materials up to 1 nm. For example, the thickness of the human hair varies between 50000 nm to 80000 nm. Nanotechnology have various and important application especially in the research area therefore it become a key technology, and already many countries invested millions of dollar in such type of technology research. Nanotechnology describes many major issues such is environmental impact and toxicity of nonomaterials [10].

The concept which leads to developed nanotechnology was firstly introduced in 1959 by Richard Feynman in his talk entitled “there is plenty of room at the bottom”, and it was known by Norio Taniguchi in 1974 [11]. The first book “engines of creation” was published in 1986 on nanotechnology by Eric Drexler, and first journal was published in 1990 by Chris Paterson. Scientist focused on nanotechnology due to progressively increases its applications day by day and is positively affected on our daily life.

1.4.1 Synthesis approaches of nanotechnology

In order to investigate the physical and chemical properties of nanostructure materials synthesis and fabrication of nanomaterials is the first and important step in nanotechnology. There are two main approaches for the synthesis of nonomaterials [12].

- Top-down approach
- Bottom-up approach

1.4.1.1 Top-down approach

In top down approach the bulk system of a material break down into its compositional sub-system. Top down approach start from bigger element, and change it into very small segments. The production of integrated circuit is the useful application of top-down approach [13]. Top-down approach refers many synthesis techniques to get nanostructure materials. Ball milling method, lithography process, nano-fabrication by printing and nano-fabrication by skiving are the typical conventional and unconventional techniques of top-down approach in making nanostructure materials. Beside these, there are some big problems come to facing by using this technique, unavailability, not excess able and main problem is its expensiveness.

1.4.1.2 Bottom-up approach

The inversion of top-down approach is known as bottom-up approach. In bottom-up approach, materials are build-up of from smaller components i.e. cluster-by-cluster, atom-by-atom, or molecule-by-molecule to form multiphase assemblies [14]. Bottom-up approach is commonly used for the synthesis of nano-materials. This approach is just the copy of nature, in which cells; crystals are produced by using this technique. By using this technique nanostructure materials are easily synthesized as compared to top-down approach because it is an easy, low cost, simple and an approachable method from top-down technique.

Chemical co-precipitation method, sol-gel method, hydrothermal method and chemical aqueous method are the examples of bottom-up approach. These two approaches are diagrammatically illustrated in figure 1.1.

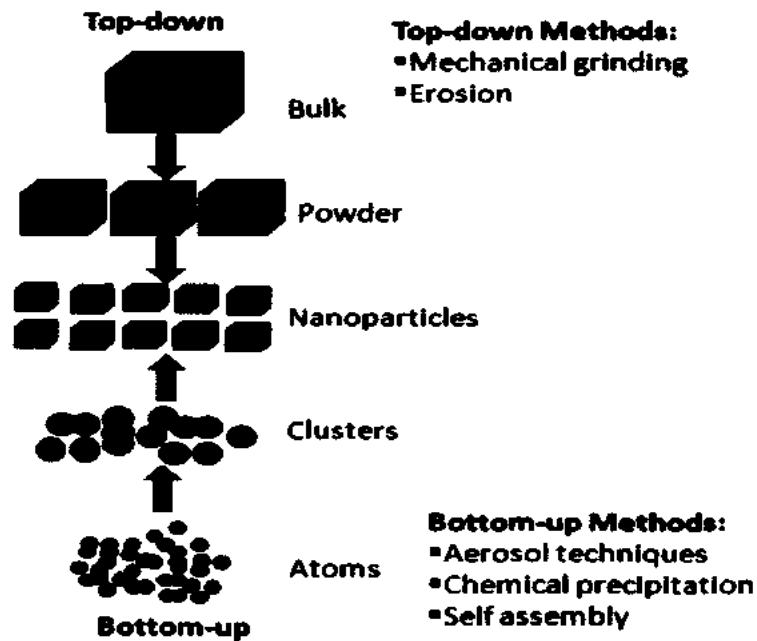


Figure 1.1: Schematic diagram of top-down and bottom-up approaches [12].

1.4.2 Applications of nanotechnology:

Nanotechnology has, unique and efficient properties especially in research area which are already discussed above in detail, due to these properties it have very wide application in our daily life.

- i. Nanotechnology is use at industry level to increase the growth ratio of the products [15].

- ii. By using different nano-techniques to mix nanoparticles with fluids to enhance drilling speed of the tools.
- iii. The drilling tools are coated with nano layer to increase their life time.
- iv. Nanotechnology is frequently used in oil industry to increase the output of extracted oil up to 50% [16].
- v. Nanocoating on bulk materials produces non-corrosive materials.
- vi. Water molecules are separated very effectively from oil by using nanotechnology approach.

Beside these, nanotechnology gets more concentration on wide range due to its beneficial application in energy conversion. The efficiency of solar cell surprisingly increased from 20% to 90% by using this technology. Also it can be use for health care treatment, medical sciences and give result for environmental protection [17-18].

1.4.3 Classification of nanomaterials

Due to its distinction application nonomaterials are classified in to three types.

- 1) Zero dimensional nanomaterials
- 2) One dimensional nanomaterials
- 3) Two dimensional nanomaterials

1.4.3.1 Zero dimensional nanomaterials

It is that type of nanostructure materials that having their all the three dimension in nano range is called “zero dimensional nanomaterials”. In general the dimension of the nano-materials is considered in the range between 1 to 100nm. When the dimension of the nanomaterials is small comparable to De-Broglie wave and quantum effects are observed, then such types of materials are in zero dimensional range. Quantum dots and quantum sphere are the examples of zero dimensional material.

1.4.3.2 One dimensional nanomaterials

One dimensional nanostructure materials can be define as “those type of materials which having its two dimensions in nanometer range and other one is not to be restricted in nanometer are called one dimensional nonmaterial's”. Nanorods, nanowires, and nanofibers all are the example of one dimensional nanostructure materials.

1.4.3.3 Two dimensional nanomaterials

Nanostructure materials which having one dimension in nanometer range while the other two dimension are not to restricted in nano size are called two dimensional nanomaterials. Quantum wall is the example of two dimensional materials.

1.5 Metal oxide

The crystalline materials which have metal cations and oxygen anion are called “metal oxide”. It has very vast application and plays a key role in many research areas of physics, chemistry, and materials science [19-22]. The metal elements react with oxygen and can form a number of various oxide compound by using different synthesis technique. The reaction between metal oxide and water cause basis and when react with acid form salt [23]. The grain size of metal oxide is generally lies in micron range but they considered as a particle whose size is greater than micron range. The metal oxides in nanometer range have great importance and various applications then other bulk metal oxides. But it is very difficult to control their size in nanometer range and it is a big issue for material science [24].

Although, metal oxide in nanometer range show different structure such as metallic, semiconductor or insulator character due to having different electronic properties. The diversity of quality of metal oxide allow the large application in the production piezoelectric devices, sensors, fuel cells, microelectronic circuits, coatings against corrosion and as a catalyst. For example all catalyst contains an oxide as active phase, supporter which permits the active element to disperse on it. Catalysts that contain oxides are employed to control the environmental pollution, and remove CO, NO_x, and SO_x species generated during the combustion process of fossil fuels [25]. Besides this, the most important areas of metal oxides are to use as a semiconductor. Therefore the majority chips used in computers have an oxide component. Furthermore, there are enough and many useful applications of such type of material under regular investigation and new methods have been introduced for synthesis [26].

Metal oxide created a center of attention in nanometer range due to its distinctive and various properties that using in many research areas [27-31]. To synthesize such types of nanomaterials a numerous techniques have been reported that can be explain as physical and chemical method. In general, there are two approaches one is top-down and other one is bottom-up approaches which contain liquid-solid or gas-solid transformation [30-32]. Furthermore, the surface of these materials can be functionalized and modify its structure. The approachable

thermal stability and chemical condition of these inorganic materials enable them to be mostly used in different field.

1.5.1 Metal oxide in nature

To date, almost 60 biomaterials have been investigated to use it for different necessary purposes. Up to now, more than 60% materials from these are reported to used it in various field either for water molecule, hydroxyl moieties treatment enable them to release ion slowly in to the solution [33]. Metal oxides play an important role and act as a fundamental stepping-stone in the growth of nano-materials. Oxides material shows their characteristic in between semiconductor and insulator because they have low free energy states as compared to metals in the periodic table [34]. Metal oxides, such as SiO_2 and Al_2O_3 are act like an insulator and are frequently used for catalysis and are non-reducible oxides. Semiconductors metal oxides provide different templates for gas sensors [34].

The observed properties related to metal oxides in technology are unchanged so far that observed in natural systems. Nature has a tendency to produce metal oxides nonomaterial in a particular way under ambient conditions. Finding the magnetic direction device magnetoatic bacteria (MTB) is the example of defined materials [35].

Chapter No. 2

Literature review

2.1 Molybdenum trioxide

Molybdenum trioxide (MoO_3) is inorganic, thermodynamically stable transition metal oxide. MoO_3 , between the other transition metal oxides represent different, unique and interesting structural, optical, electrical and chemical properties. MoO_3 is a semiconductor metal oxide having wide band gap 2.95 eV in bulk while 2.99 eV in nanostructure size. MoO_3 use as a cathode material in the formation of high-energy storing charge solid-state micro batteries. It exhibits photo, electro, gas chromic effects and use as an electrochromic material to get great interest for the formation of electronic displays, smart window technology and optical coating switching coating. Nanostructure and thin film of Molybdenum trioxide have also great application in the development of sensors and lubricants [36].

Molybdenum trioxide like other metal oxide has different oxidation states, ranging from 1^+ to 6^+ . In MoO_3 the oxidation state of molybdenum “Mo” is 6^+ . The oxidation states of the “Mo” atom are decreases by reduction of the oxygen partial pressure. In MoO_3 , the reduction of oxygen can be accommodated by the compensation of two oxygen atoms in the stoichiometric defects inside the crystal structure [37-38]. Lower ratio of oxygen to metal, there are seven stable and meta-stable sub-oxides are formed $\gamma\text{-Mo}_4\text{O}_{11}$, $\eta\text{-Mo}_4\text{O}_{11}$, Mo_5O_{14} , Mo_8O_{23} , Mo_9O_{26} , $\text{Mo}_{17}\text{O}_{47}$ and $\text{Mo}_{18}\text{O}_{52}$ due to the composition of MoO_3 and MoO_2 [39].

Commonly MoO_3 has three phase namely orthorhombic ($\alpha\text{-MoO}_3$), monoclinic ($\beta\text{-MoO}_3$) and hexagonal (h-MoO_3) here in our thesis work we are interested in hexagonal molybdenum trioxide (h-MoO_3) crystal structure.

Hexagonal molybdenum trioxide (h-MoO_3) has interesting and wide application especially in solar cell and can be use as a p-type as well as n-type materials in the solar cell device. The synthesis procedure is discussed in detail in chapter 3.

2.1.1 Physical properties of MoO_3

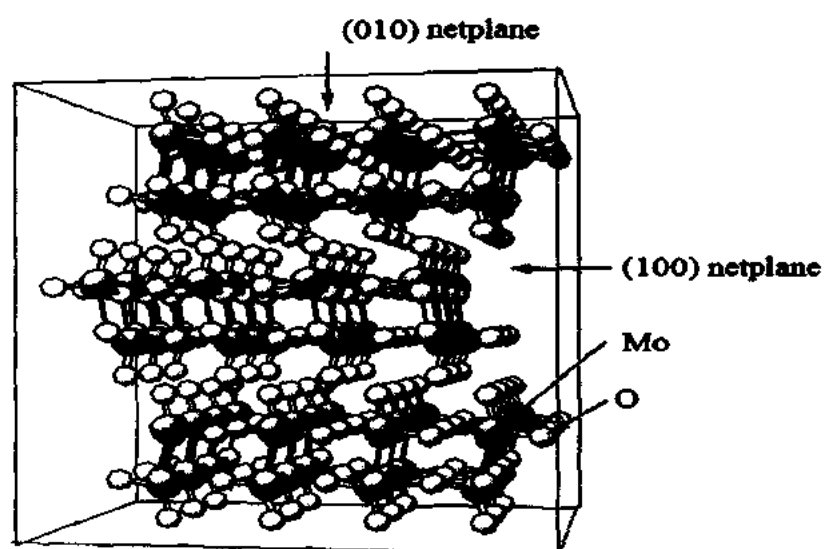
Molybdenum trioxide (MoO_3) is a chemical compound formed from molybdenum “ Mo^{+6} ” and oxygen “ O^{-2} ”. This compound is fabricated on large amount from any other molybdenum compound. The physical properties of MoO_3 are illustrated in table 2.1.

Table2.1: Physical properties of Molybdenum trioxide (MoO_3).

Molecular formula	MoO_3
Molar mass	143.93g/mol
Crystal structure	Bcc
Appearance	Yellow or light blue solid
Order	Order less
Density	4.69g/cm^3
Boiling point	1155°C
Melting point	755°C
Band gap in bulk form	2.95 eV
Solubility in water	0.1066 g/100mL (18°C)

2.1.2 Structure of MoO_3

In solid state, the MoO_3 shared with hydrous molecule to produce octahedral MoO_3 in orthorhombic crystal. The chain of the oxygen atoms are formed due to sharing the edges of octahedral structure and form the layers. These octahedral layers contain single short molybdenum-oxygen bond and also have non-bonding oxygen atom [40]. Figure 2.1 shows the crystal structure of MoO_3 .

**Figure 2.1:** structure of MoO_3 [41]

2.1.3 Optical properties of MoO₃

The electronic structure and electrical properties of nanostructure molybdenum trioxide are not examined in details; however there is a common trend that increasing the concentration of metal with oxygen the electronic conductivity of the materials increases. The calculated optical band gap of the molybdenum trioxide is 2.95 eV in bulk size while 2.99 eV in nanometer range. The band gap of the MoO₃ can be reduced by introducing some impurities level near with conduction band or by the reduction of oxygen atoms, then it acts like a semiconductor. The change in the electronic conductivity of the insulating MoO₃ to the semiconducting Mo₁₈O₅₂ varying in the range of ($\rho = 78.1 \text{ } \Omega/\text{cm}$) to metallic $\eta\text{-Mo}_4\text{O}_{11}$ ($\rho = 1.66 \times 10^{-4} \text{ } \Omega/\text{cm}$). The anisotropic change in the crystal structure exhibits different electronic properties, however exact data on these determinations are not available [42].

Molybdenum trioxide is a semiconductor materials having wide band gap 2.95 eV already showed in table 2.1. It is found normally in white or light gray colored in powder form and changed its color turn to blue when the excitation of electron take place inside it. Generally, the crystalline form of the MoO₃ are found to be in monoclinic structure ($\beta\text{-MoO}_3$) or orthorhombic structure ($\alpha\text{-MoO}_3$) both these structure are fundamentally formed due to corner-sharing of MoO₆ octahedral. Monoclinic phase represents amorphous nature of MoO₃ especially in thin film, which shows valuable chromomeric properties as compared to crystalline nature of thin film or a single crystal [43].

The thin films of insulator compounds of metal oxide are used in large scale, such as by preparing semiconductor devices. i.e. integrated circuits and transistors. Fabrication of molybdenum trioxide thin film in metal oxide is very complicated by thermal evaporation process, because of the lower vapor pressure of the essential atoms which takes part in the reaction. So, such types of evaporated film may frequently possess an excess of metal atoms, which changes the electrical properties of the film and act as a doping element. This doping element contains a low ratio of one molecule per million molecules of the order 10^{17} cm^{-3} . The impurity changed the energy diagram of the doped thin film as compared to un-doped thin film [40].

2.1.4 Nanostructure properties of MoO₃

To study the properties of MoO₃ at nanometer range are very interesting, due to its unusual chemistry and unique electronic structure by its various oxidation states. Different metal

oxides are synthesized spontaneously over self-assembled method with monolayer, which is applicable for heterogeneous catalysis. Synthesis of MoO₃ at nano size shows large activity to formed stable environment to develop the required oxidation states and isomerism of hydrocarbons, and provides appropriate support for intercalation cathodes. Thermodynamically stable (α -MoO₃) phase is formed due to bi-layered arrangement of octahedral MoO₆ sharing its corner and bonded together by covalent forces. It is also used in transmission electron (TEM) for the image calibration, but currently available in bulk form [44].

Beside this, MoO₃ exhibits promising properties is used as a catalyst. The semiconducting thin film of MoO₃ recently gets more interest, because of their useful application in conductance type gas sensors. MoO₃ thin film is very sensitive for different gases like CO, H₂, NO, NO₂ and NH₃ at low temperature 300° C as well as at high temperature 600° C. But the working temperature can be maintained below from melting point of MoO₃, because there is also a chance for the grain growth of other polycrystalline materials. The properties of the synthesized thin film are dependent on deposition parameters and deposition technique. Therefore, a number of techniques are investigated to optimize structural and functional properties of the desire thin film. One dimensional nanostructure of MoO₃ is reported in a lot of publications, because they contain novel characteristics of large surface area. The conductivity is strongly enhanced due to surface reaction and the crystallinity level decreases up to possible instabilities [45].

2.1.5 Applications of MoO₃

MoO₃ has wide application especially in research area due to its unique, interesting and distinctive properties. Molybdenum trioxide is used for the preparation molybdenum metal, which is further used for the manufacturing of steel and other corrosion-alloys. The conversion of MoO₃ in to “Mo” metal requires a suitable treatment with hydrogen at appropriate temperature.



MoO₃ is also considering as a component of co-catalyst and used for the production of acrylonitrile by the oxidation of ammonia and propane at industry level [46]. Molybdenum trioxide is also used as an anti-microbial agent such as in polymers, when react with water it generate H⁺ ions which give result to kill bacteria effectively [47].

Molybdenum trioxide has vast application and used at large scale in industry to increase the product effectively. It is also used for the preparation of molybdenum products at industry level. It is obviously used in industry as a catalyst, a crop nutrient, a pigment, a flame retardant for polyester, a component of glass, polyvinyl chloride, and ceramic also used as a chemical reagent. Besides these, MoO_3 thin films are used as a p-type semiconducting oxide material in photovoltaic cell and its resistance is greatly affected by the presence of gases [48].

2.1.6 Molybdenum trioxide used as a catalyst

Molybdates and vanadates are commonly used on large scale as partially oxidative catalysts [49]. However, commercially pure MoO_3 is of limited importance and always consider is the major component of the imperative industrial catalysts. Methanol oxidation $\text{Fe}_2(\text{MoO}_4)_3$, V-Mo-O [50], oxidation and ammo oxidation of propane are the some examples of catalysts. But MoO_3 has simple structure and used in large scale at industry level as compared to other multi component Molybdates, also having some natural catalytic properties and usually studied as a model oxidation catalyst [50-51]. The catalytic study of methanol (MeOH) for partially oxidation has been the target of the previous investigation [52]. MoO_3 is widely used (up to 100%) as a catalyst for partial oxidation of (MeOH) changed to formaldehyde [49]. It has been reported that the reaction is surface structure sensitive; therefore it is not clear that the surface plays a mechanistic role in the reaction. So, therefore the structure-reactivity relationship of MoO_3 is not investigated [50].

2.2 Literature review

S. S. Mahajan *et al.* [18] studied the properties of MoO_3 and showed the importance of the transition metal oxide since from last two decades due to its various interesting properties and having unique structure. Metal oxides have wide application especially in the research area of physics, chemistry, energy conversion and nanotechnology. MoO_3 use as a cathode material in the generation of high energy solid state micro-batteries. It is also use as a promising electrochemical material and show electro, gas, photo chromic effects. Due to having such types of properties, MoO_3 has uses in the generation of electro chromic display devices, smart window technology, display devices and optical switching coatings.

Nirupama V *et al.* [68] prepared the thin film at low temperature and also showed various application of molybdenum trioxide in different electronics devices. MoO_3 is an interesting material due to its vast range of stoichiometric applications, with attractive behavior including

catalytic and chromomeric properties. Furthermore, it is used in the development of optical memories, electrochromic display devices, lithium ion batteries and gas sensors. MoO_3 film can be fabricated with different methods for various purposes including thermal evaporation, Chemical vapor deposition, electron beam evaporation, electro deposition, sputtering, pulsed laser deposition and sol-gel process. For the synthesis of MoO_3 thin film dc magnetrons sputtering method is used on large scale even at industry level practiced method. By using this method thin film can be fabricated at low temperature and also control the chemical compositional ratio on large area of the substrate.

Lee S. H *et al.* [73] describe the properties of transition metal oxides that changes with temperature, size, and coloration etc. Transition metal oxides (MoO_3 , V_2O_5 and WO_3) exhibit unique properties and vast application in the field of electrochromic and batteries. The electrochromic property of the transition metal oxides refer them to use in the synthesis of displays and smart window. The fabrication of smart windows is greatly affected by changing the heating and cooling conditions. The growth of electrochromic devices can be enhanced by increasing the efficiency of coloration and also depends to decrease the coloration reaction time. Since from last two decades the main focused on the fabrication of metal oxides at nanoscale and also to enhance their properties. The expectation from such small size scales that to increase the progress of switching times and amplification of electrochromic response depends on the reduction of diffusion length and increased the surface area. Beside this, these materials are used in energy storage system to increase energy stored per unit mass, and also develop the structural stability over various charge cycle. Transition metal oxides are used as a cathode material in rechargeable batteries. It is found that the chemical structure and particle size greatly change the final energy density and power performance.

Angamuthuraj *et al.* [86] showed the synthesis of hexagonal molybdenum trioxide (h- MoO_3) by solution based chemical co-precipitation method. Verification of crystal structure is confirmed by the study of (XRD) analysis that the powder had a metastable hexagonal structure. The identification of characteristic vibrational band of Mo-O was confirmed by Fourier transform infrared spectroscopy (FTIR). They studied the size, shape and surface morphology of h- MoO_3 by scanning electron microscopy (SEM) and Transmission electron microscopy (TEM) respectively. The surface morphology study clearly showed that the powder contains one dimensional (1D) hexagonal rods. They studied the Electron energy loss spectroscopy (EELS)

which clearly showed and confirm the characteristic peaks of Molybdenum and Oxygen. Thermogravimetric (TG) analysis confirmed that hexagonal phase of MoO_3 stable up to 430°C when the temperature increases from this ranges the phase is changes to orthorhombic phase structure. The transmittance and reflectance behavior was studied by means of UV-visible spectroscopy and the optical band gap energy was found from Kubelka-Munk (K-M) function and the estimated value was 2.99 eV. Approachable research methods have been interested on the synthesis of metastable nano crystalline materials due to their distinctive and remarkable improved properties as compared to their bulk structure. Synthesis of metastable nano crystalline material is always a big problem with controlled size and shape, but the properties of the nano-materials are inter-connected with their size, shape and chemical composition.

Ye Zhao *et al.* [52] presented the synthesis of Molybdenum trioxide (MoO_3) at nanostructure by using direct oxidizing spiral coil of molybdenum metal at specific atmosphere. The reported method is very simple in which the current is passing through the coil. They showed that the synthesis of the thin film can be fabricated at low temperature of the substrate (normally below 200°C), and also different structure can be formed by changing the current of the coil and temperature. They reported that by adjusting the current through the coil the thickness and size can be reduces of $\alpha\text{-MoO}_3$ and $\beta\text{-MoO}_3$, and can be synthesized in nanometer range at specific atmosphere. The optical band gap related to these nanostructure materials has greater value i.e. 2.99eV as compared to that of bulk material. Photoluminescence of such type material at low temperature is about 395nm. This method provides a simple, sophisticated way to synthesize metal oxide nanostructures and increased their interest.

Objectives

The objective of the present work is to grow and study the crystal structure, phase, surface morphology of molybdenum trioxide (MoO_3) at nanometer scale. The first goal was to synthesize (MoO_3) in hexagonal phase nanostructures by using chemical co-precipitation method. The X-ray diffraction studied conformed the phase and meta-stable hexagonal structure of synthesized MoO_3 . Second goal was to examine the morphological changes of the nanostructures with different reaction conditions. The main and final goal was to tune the optical properties and band gap of the MoO_3 using Chromium doping.

Chapter No. 3**Synthesis and structural characterization**

To prepare hexagonal phase molybdenum trioxide (h-MoO₃) nanorods several methods have been used. Here only two methods are introduced and explained briefly.

3.1 Sol-gel method

Precipitates which are synthesized in the form of colloidal, suspended in liquid are called "Sol" and the semi-hard form of the colloidal is known as "gel". Supercritical treatment of gel is known as "aero-gel". It is hard and dehydrated material made of small pore of size approximately 100nm. Further treatment of aero-gel at proper temperature it becomes "xero-gel". It looks like a solid material and its pore size varies in the range 1 to 10nm.

Sol-gel method is the most popular and a multi steps method which is used for the fabrication of metal oxide nanostructure [53]. This method concerned with wet chemical route technique normally starts by mixing of metal salts in suitable solvent at required temperature [53-54]. By controlling parameter in sol-gel process such as pH value which is controlled from the start of the reaction to get homogeneous precipitate and gel of the solution [55]. Acid and bases are added to the solution to get required pH value of the solution, different type of acids and polymers are used with metal ions to form "sol" as well as to control size and consistency of the product [55-59]. By introducing the carboxylic acid with metal ion it forms in to essential ion gel [60]. The gel is further more heated at 150 to 300 °C to remove unstable organic component water etc. To obtained the single phase nano crystalline structure of metal oxides the gel powder is dried up to 400 to 800 °C and also depend on the nature of the chemical [61-62].

This method is mostly used for the preparation of colloidal dispersions of numerous materials which posses' organic material, and also having organic- inorganic hybrid materials [53]. The synthesized colloidal dispersions due to this method are further used to fabricate fiber, nano powders and thin films. In this process, firstly the solution is hydrolyzed with water and then allowed to condense to get precipitate of metal oxide nanostructure. In next step, the obtained precipitate is too washed, dried and grinded to get the fine crystalline nanostructure. Hydroxylation plays a main role in the formation of metal oxide nano structure, and using this process the following major problems can be controlled.

- When two hydrolyzed react with one another they make a water molecule.

- When two opposite species reacts mean (hydrolyzed and unhydrolyzed) with one another in the result alcohol molecule are formed.

The properties of finally synthesized products changed and greatly affected by changing the rate of hydrolysis and condensation. Smaller and fine particles are fabricated by using slow and controlled hydrolysis process. While denser and big particles are fabricated by using base-catalyzed condensation process.

3.1.1 Steps in sol-gel method

Sol-gel process is an easy method and can performed in four steps is given below.

- Preparation of solution to formed gel (including hydrolysis and condensation process).
- Aging
- Drying
- Heat treatment

3.1.2 Applications of sol-gel method

- Sol-gel method is broadly used to fabricate different type of materials, such as gel, glasses, amorphous and powder etc.
- Sol-gel method is used for the synthesis of thin film and nano particles.
- It s used to get ceramics and monoclinic membrane.
- It has great application by using it in optics and electronics.

3.1.3 Advantages of Sol-gel method

- It is an easy, low cost and an approachable method.
- It can perform at low temperature.
- In this method chemical reaction can be controlled compositionally.
- By using this method impurities can doped in feasible way.

3.2 Co-precipitation method

Co-precipitation method is mostly used for the synthesis of different nanostructure materials. This method is used in large scale as compare to all other methods due to its efficient application. In this method metal cations from ordinary medium are precipitated typically such as hydroxide, carbonates, formates, oxalates [63-65]. In this method the precipitates are consequently treated at proper temperature to acquire resultant products in powder form. To get homogeneity, the mixing ratio of the precursor elements must be closer to each other [66].

In co-precipitation process the solubility ratio at atomic scale and required low temperature for the synthesis of nanostructure materials [67]. For the synthesis of nano structure material there are various technique are reported in literature, but each synthesis technique require its own conditions i.e. pH, homogeneity, precursor reaction etc. However co-precipitation method require some condition to synthesize the resultant product in nanostructure size such as to control pH, temperature, concentration of the solution and stirring speed of the mixture all these conditions are involve in co-precipitation method [68-69].

3.2.1 Advantages of Co-precipitation method

- It is simple and direct method for the synthesis of metal oxide, and has great reactivity at low temperature sintering.
- It is an easy and an approachable method even it can be perform at room temperature.
- Homogeneous solutions of the reactant precipitate refer it to low temperature.

3.2.2 Disadvantages of Co-precipitation method

- This method is not suitable for the synthesis of metal oxide at high temperature.
- This method is not applicable for different growth rate of precipitate and also having different solubility rate of the reactant.

The present work demonstrated the synthesis of molybdenum trioxide on chemical based co-precipitation method. This method is used on large scale for the synthesis of nanomaterials, because it has various applications. It is an easy, inexpensive, low temperature and an approachable method for the synthesis of metal oxide at nano structure.

3.3 Sample preparation

Chemical based Co-precipitation method was used to synthesize h-MoO₃ nanorods in powder form. In which Ammonium heptamolybdate tetra hydrate (AHMT) was dissolved in distilled water and HNO₃ was used to make the precipitation of the solution (salt form). The series of samples of pure MoO₃ and chromium doped MoO₃ were prepared in the same way by same molarity, but only the temperature of the reaction was varied while all other parameters were kept constant. Now for Chromium doping, Chromium chloride (Cr_{III}Cl₃) was added to the solution with different concentration and a series of samples (0.5wt. %, 1wt. %, 2wt. %, 3wt. %, 4wt. %, and 5wt. %) were obtained.

3.3.1 Chemicals

Following chemical were used for the synthesis of pure h-MoO₃.

- 1) Ammonium heptamolybdate tetra hydrate (NH₄)₆Mo₇O₄H₂O
- 2) Nitric Acid (HNO₃)
- 3) Distilled water (pH value 6)

3.3.2 Synthesis of h-MoO₃ nanorods

The experiment was performed in step wise at 25° C temperature. Pure h-MoO₃ samples were also prepared at 40° C temperatures, while the reaction was carried at temperature ranges from 100° C to 1455° C, when placed in oven. The whole experiment may be performed in the following steps.

Step 1:

In step first, to get 0.2M concentration of the solution, Ammonium heptamolybdate tetrahydrate (AHMT) having weight 4.94g/mol was added in 20ml distilled water of pH value 6 at 25° C temperature. The solution was stirred with the help of hot plate and magnetic stirrer up to 15 minutes to dissolve AHMT in distilled water. After stirring process, AHMT was completely dissolved and observed at a transparent solution.

Step 2:

In second step 5ml Nitric acid was mixed drop wise and gradually into the precursor solution and observed the precipitate of the solution immediately. To get the homogeneity of the solution, it was stirred again for 10 min.

Step 3:

Then the solution was placed in Lab tech at 85° C for 1 hour, which was the reaction temperature of the solution.

Step 4:

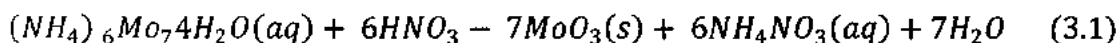
Then the resultant precipitate was separated from the mother liqueur and washed several times carefully with distilled water of pH value 6. The resultant precipitate was centrifuged at the rate of 5000 rpm and the acceleration was 6.

Step 5:

After completing the washing procedure, the precipitate was placed in vacuum oven pump for drying at 70° C for 6h.

Step 6:

Finally to grained the hard and dry precipitate with the help of “pistol mortar” to get white powder of the resulting products. At the ends chemical based co-precipitation method was used to synthesis h-MoO₃ nanorods in powder form according to the following equation.



The crystallinity and phase decomposition was analyzed by means of XRD in the range of 5 to 60°. The surface morphology and size of the crystal was examined by means of scanning electron microscope (SEM) with various magnifications. The optical properties of the h-MoO₃ were analyzed by DRS and spectra was recorded by means of computer controlled T90+UV-vis spectrometer.

I also prepared the Chromium “Cr” doped h-MoO₃ nanorods in powder form in the same way with different doping concentration from 0.5wt. % to 5wt. %, and was characterized with the same techniques which will be discussed briefly in next chapter.

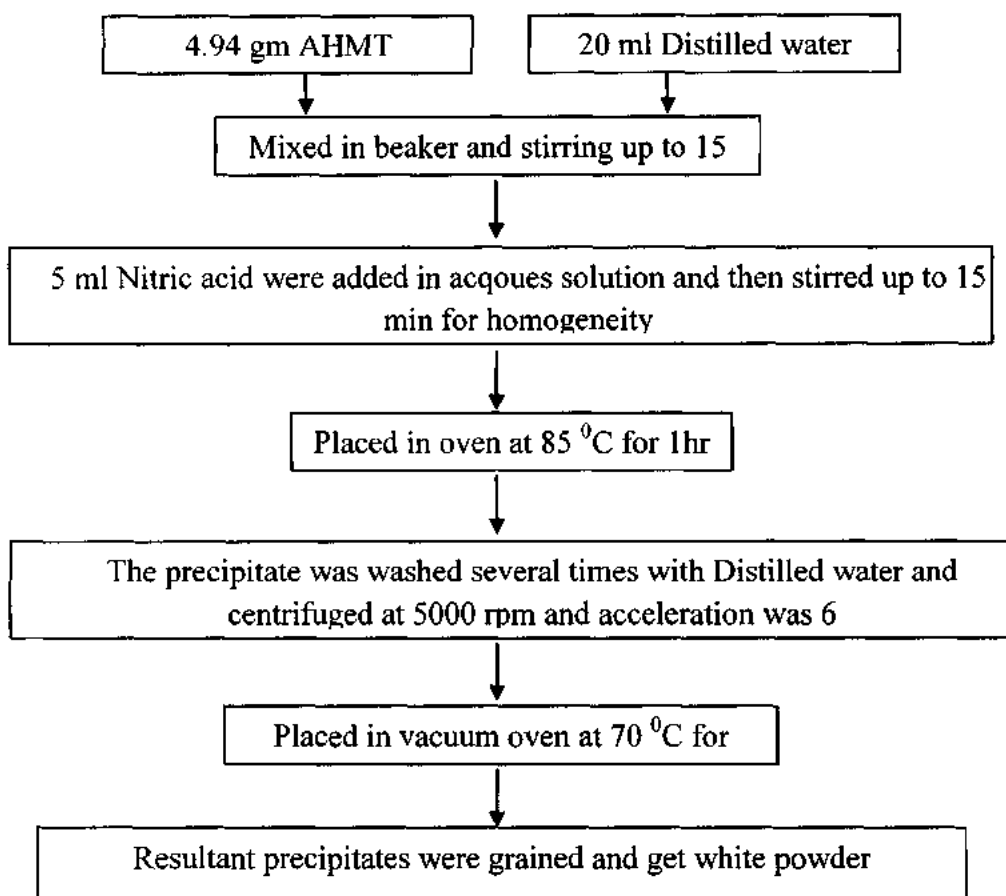


Figure 3.1: Flow chart for preparing pure MoO₃ nanorod.

3.4 Characterization techniques

Experimental techniques are used to examine the properties of the synthesized material such as crystal structure, phase decomposition, surface morphology, shape and size of the particles, compositional analysis, and optical study of the material. For that X-ray diffraction (XRD), Scanning Electron Microscopy (SEM), Energy Dispersive Spectroscopy (EDX) and Diffuse Reflectance Spectroscopy (DRS) have been employed to examine the above property respectively. The detail of these characterization techniques are given below.

3.4.1 X-ray diffraction

XRD technique is broadly used to study phase composition, crystal structure, quality, lattice parameter, and also used to determine the crystallite size of the material [70]. Because every material has unique XRD pattern act like a finger print of the materials, and gives information about the material that how the atoms are arranged inside it. Furthermore XRD can characterize both types of samples either in powder form or in solid form [71]. XRD technique differentiates many phases of the same crystal structure, and analyzes the crystal structure of different material [72]. XRD technique is based on diffraction phenomenon, that X-rays are diffracted from regular arranged crystal planes of the materials. In 1912 W.L Bragg explained the diffraction phenomenon very well that “the diffraction occur only if the planes of the crystal act like a mirrors when X-ray fall on it” this law is known as Bragg’s diffraction law [73]. Bragg’s law is explained graphically in Figure 3.2.

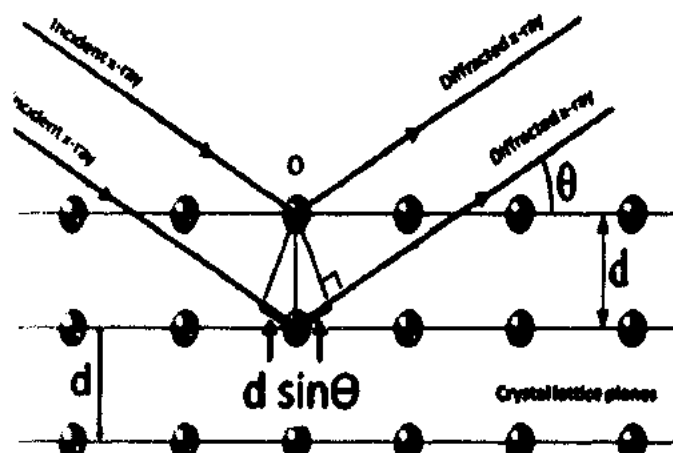


Figure 3.2: Bragg’s reflection from parallel planes [74].

Mathematical form of Bragg's law is given below;

$$2d\sin\theta = n\lambda \quad (3.2)$$

Where, θ = Diffraction angle

λ = Wavelength of X-ray

n = Integral number

d = Inter atomic planer distance

But here in this work the XRD technique is used to examine the crystal structure, phase decomposition and also calculated the crystallite size of the samples.

3.4.2 Working principle of X-rays diffractometer

The X-ray diffractometer (Model D-8 Broker Company Ltd) operated at 40kv and 25mA was used to verify the crystal structure and size of the particles. In X-rays diffractometer Cu- α_1 (1.54 Å) is used as an X-rays source. A sample holder "S" in the form of flat and round glass slide (2.5×5cm²) rotating perpendicularly to the plane of the axis labeled "O" is made possible. The monochromatic X-rays beam is incident on the specimen placed in the sample holder. The specimen reflects X-rays with specific intensity, and is recorded through a detector which is fixed opposite to the X-ray tube. Initially X-rays source, counter and specimen all lies in the same plane (coplanar). The XRD pattern was taken in the range of 5 to 60⁰, where 0.5⁰ was the angle increment and the given stay time was 2 Sec.

The angular position of the counter was measured in term of "2 θ " not only single " θ " and marked it on a graduated scale. The incident angle and reflection angle should be equal to each other because the specimen and carriage are adjusted mechanically to each other. The rotation of the specimen through angle " θ " is accompanying by a "2 θ " rotation of the counter. Incorporate collimators are in a job in the path of X-ray to produce well defined, monochromatic and focused beam. The counter moving at constant angular velocity recorded the diffracted beam intensity as a function of "2 θ ".

3.4.3 Calculation of the average crystallite size

With the help of Debye Scherer's formula we can calculate average crystallite size of the crystal, and is given below.

$$D = \frac{k\lambda}{\beta \cos\theta} \quad (3.3)$$

Where “ λ ” is the wavelength of the XRD radiation, θ_β is the Bragg’s diffraction angle, where “ k ” is the shape factor has constant value (0.9) and “ β ” is the full width at half maximum of the observed diffraction peak. The average crystallite size is calculated by taking the high intensity diffracted peaks of the observed spectra [75-76].

3.4.4 Calculation of particle size

Consider that “ t ” is the thickness of the crystal measured perpendicularly to the reflecting planes. Let there be $(m+1)$ reflecting planes which reflect the X-ray beam with varying angle called “ θ_β ” satisfying the Bragg’s law with constant wave length “ λ ” and in valued inter atomic space “ d ” between the planes. That is

$$\lambda = 2d \sin\theta \quad (3.4)$$

Where $m = 1$ for maximum intensity

Now if “ θ_β ” is made by the incident rays with the reflecting planes, then all the scattered rays will be the integral multiple of the wave length ($n\lambda$). It shows that all the diffracted rays obey the Bragg’s law and are constructively interfere, while the remaining rays which are not reflected are destructively interfered, cannot obey the Bragg’s law. The maximum reflection with high intensity recorded Vs “ 2θ ” is shown in Figure3.2.

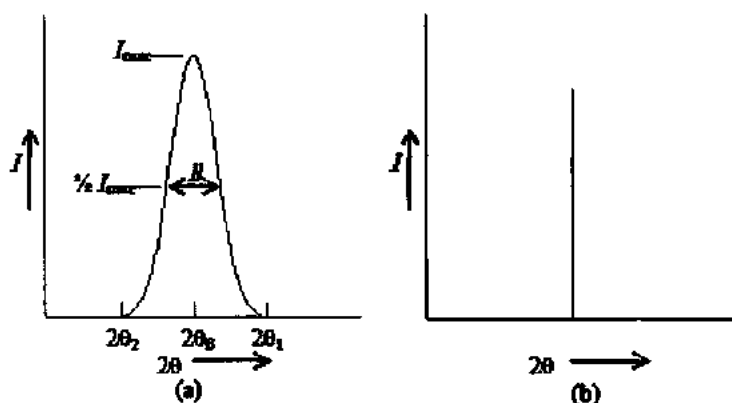


Figure 3.3: Particles size on diffraction curves.

In Figure 3.3 (a) width of the curve illustrates the thickness of the crystal and vice versa, when the width of the curve increases than the thickness “ t ” decreases. The “ β ” is measured in radian is called Full width at half maximum (FWHM) of the intensity. The width “ β ” is angular

width in terms of “ 2θ ” not single “ θ ”. There is rough approximation for width “ β ”, and half of the difference between the two extreme angles. For that we consider the triangular shape of the diffraction. Therefore

$$\beta = \frac{1}{2}(2\theta_1 - 2\theta_2) = \theta_1 - \theta_2 \quad (3.5)$$

Now here we replace the path difference “ d ” with “ t ” which is the entire thickness of the crystal rather than space between the adjacent planes.

$$2t\sin\theta_1 = (m + 1)\lambda \quad (3.6)$$

$$2t\sin\theta_2 = (m - 1)\lambda \quad (3.7)$$

by subtracting we find:

$$t(\sin\theta_1 - \sin\theta_2) = \lambda \quad (3.8)$$

$$2t\cos\left(\frac{\theta_1 + \theta_2}{2}\right)\sin\left(\frac{\theta_1 - \theta_2}{2}\right) = \lambda \quad (3.9)$$

But, the measured sum of θ_1 and θ_2 is very small and approximately equal to θ_β

$$(\theta_1 + \theta_2) = \theta_\beta \quad (3.10)$$

$$\sin\left(\frac{\theta_1 - \theta_2}{2}\right) = \left(\frac{\theta_1 - \theta_2}{2}\right) \quad (3.11)$$

Therefore

$$2t\left(\frac{\theta_1 - \theta_2}{2}\right)\cos\theta_\beta = \lambda \quad (3.12)$$

$$t = \frac{\lambda}{2\cos\theta_\beta}$$

A more exact form of this equation is by adding shape factor constant “ k ”

$$t = \frac{k\lambda}{2\cos\theta_\beta} \quad (3.13)$$

From this equation we can calculate the particle size with highest intensity observed peaks, and is known as Scherer’s formula [77].

3.5 Scanning electron microscopy (SEM)

Scanning Electron Microscopy is a nondestructive analytical technique is used by the scientist in different field i.e. for the study of surface morphology, shape and size of the material [28]. Furthermore SEM is the best way to characterize nanostructure nonomaterial. SEM scan the area of interest and produces the image on the basis of scattered electrons from the surface of

the sample is in the form of (Electronic signal) having a unique pattern, which depends on the bending of electron from surface and edges consist by the sample. SEM is a non destructive analytical technique through which we can explain the topographic study of the surface of the sample. The unique and important property of the SEM is to produce 3-D image of high resolution and with varying magnification by covering the large depth of field [79]. Figure 3.4 explained the various part of the SEM in detail.

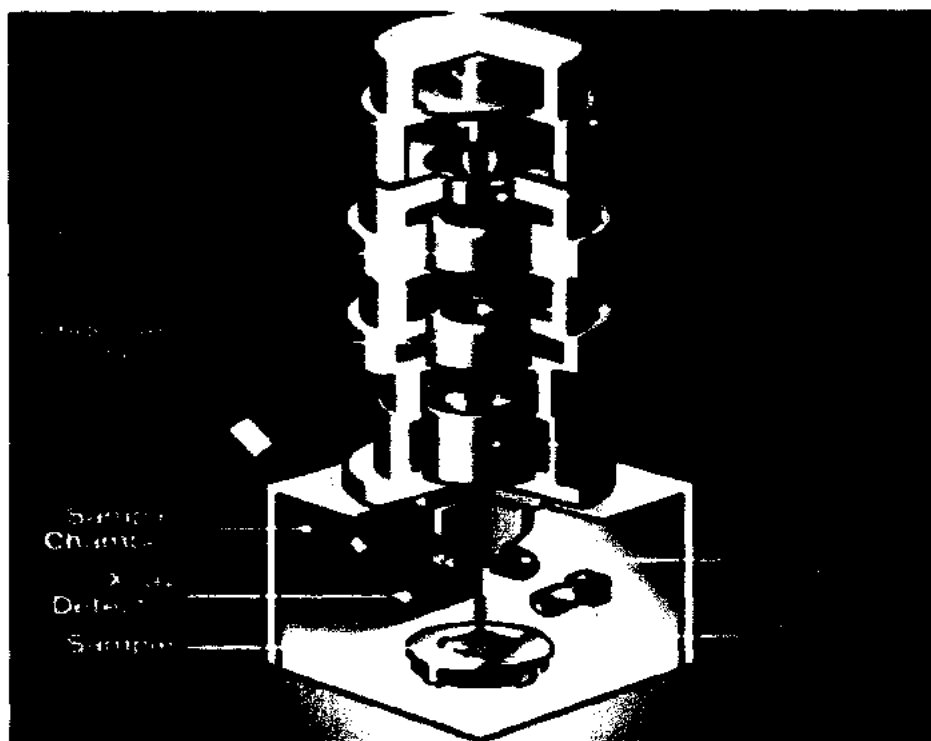


Figure 3.4: Schematic diagram of SEM [80].

3.5.1 Principle of SEM

Primary electrons having high energy produced by the electron gun fall on the surface of the sample and generate secondary and back-scattered electrons which are reflected from the surface of the sample. A detector collects these electrons in the form of (electronic signal) already installed in SEM, and used for the formation of images of the sample on the screen. Secondary electrons are responsible for image formation of the surface of the sample, therefore the intensity of the secondary electron is measured as a function of the position of the high energy (primary) electrons. The intensity of the back-scattered electrons is used to determine the atomic number of the present element in the sample. SEM gives the complete information about the topographic view of the sample by changing the intensity of the secondary and back-scattered electrons [81].

3.6 Energy dispersive spectroscopy (EDX)

Energy dispersive spectroscopy is employed to determine the chemical composition in materials. EDX is based on the interaction between high energetic electron beam and material. The high energetic electron excited the inner shell electron of the atom. The excited electron create a vacancy in inner shell, Outer shell electron of high energy comes to fill this vacancy in a result characteristic X-ray are emitted from the materials are detected by a detector. Every elements have unique characteristic X-ray and used for the identification of elements contain by the sample. because every elements emits its own family of characteristic X-ray [82].

From the EDX spectrum we can determine elemental composition of the sample and gives information about the element present in the sample.

3.7 UV/Visible spectroscopy

UV/ Visible spectroscopy is one of the most important techniques to determine the purity of the material. It is also known as reflectance or absorbance spectroscopy. The absorbance spectra can be measured at specific wavelength, which observed the impurity peaks contain by the material [83]. Absorption of light gives information about the transitions of electron from one state to another state. UV visible light fall on molecules, the non-bonding electron of the molecule absorbed the light in the form of energy and jumps to the anti-bonding molecular orbital. When the energy gap between HOMO (highest occupied molecular orbital) and LOMO (lowest occupied molecular orbital) is small, then the light of longer wave length will be absorbed by the electrons of the molecule [83]. This is very important spectroscopy for the characterization absorption, reflection and also use for transmission for different materials such as filters and pigments. Band gap of the material can be calculated by using this spectroscopy. This absorption spectroscopy is performed by using the electromagnetic radiations ranging between (190nm to 800nm). The electromagnetic radiations between (190 to 400nm) are the ultraviolet "UV" region while that of (400 to 800nm) is the visible region [84].

UV visible spectrometer is shown in figure 3.5.



Figure 3.5: Schematic diagram of UV visible spectrometer

3.7.1 UV visible working principle

UV visible spectrometer contains the following major components.

- Source (both UV and visible)
- Sample containers
- Wavelength selector
- Detectors
- Signal processor

It is very simple spectrometer and can operate in a simple way. UV visible sources produces a beam of light are comes to strike with mirror first and then passes through the slit first and moves to diffraction grating. A prism or diffraction grating is fixed inside the spectrometer in which the incoming light passes through it, the prism divide the light into its component. Furthermore, these components are again separated by using the half mirror. Each and every incident beam of light divided into two components [84]. The first component of the beam passes through sample cuvette, which has the solution of the compound. The second beam which is also known as

Chapter No.4

Results and Discussion

In this chapter the experimental results obtained during this project will be presented and discussed. Specifically crystallinity, phase decomposition, surface morphology, compositional analyses and optical properties of both the pure and doped synthesized materials are studied in detail. The following samples will be discussed in this chapter.

- 1) Pure h-MoO₃
- 2) Cr doped h-MoO₃ from 0.5 to 5 wt. %

All these samples were synthesized on the solution based chemical co-precipitation method, already mentioned in previous chapter. Here, we discussed the XRD analysis of the synthesized samples as given below. In next sections we will discuss how to achieve the pure phase and the doping effects on the physical properties of the MoO₃.

4.1 Structural phase characterization

Crystallinity and phase decomposition of the synthesized sample was determined by X-ray Diffraction (XRD) using (Model D-8 Broker Company Ltd) X-ray diffractometer with CuK α_1 1.54 Å radiation in the range of 5 to 60° in steps of 0.2/min. The typical XRD spectrum of the synthesized sample of pure (h-MoO₃) is shown in the figure 4.1. All the resulting diffraction peaks of the resulting product were easily indexed by pure hexagonal phase (h-MoO₃) with the reference to reported values (JCPDS-00-048-0399) a = 10.5 Å and c = 3.7278 Å. The observed peaks of the XRD pattern were in hexagonal phase (h-MoO₃), and were well matched with XRD reported pattern correspond to the planes (010), (110), (020), (120), (111), (021), (220), (121), (230), (041), (002), (050) and (331) respectively.

The high intensity peaks were observed at 9.799° and at 26.5° which arised from (010) and (120) planes, respectively. The high intensity and sharp peaks show that the synthesized product is well crystalline in hexagonal molybdenum trioxide (h-MoO₃) phase [85]. No other secondary impurities peaks were observed of the polymorphs of MoO₃ namely Orthorhombic (α -MoO₃) and Monoclinic (β -MoO₃) [86].

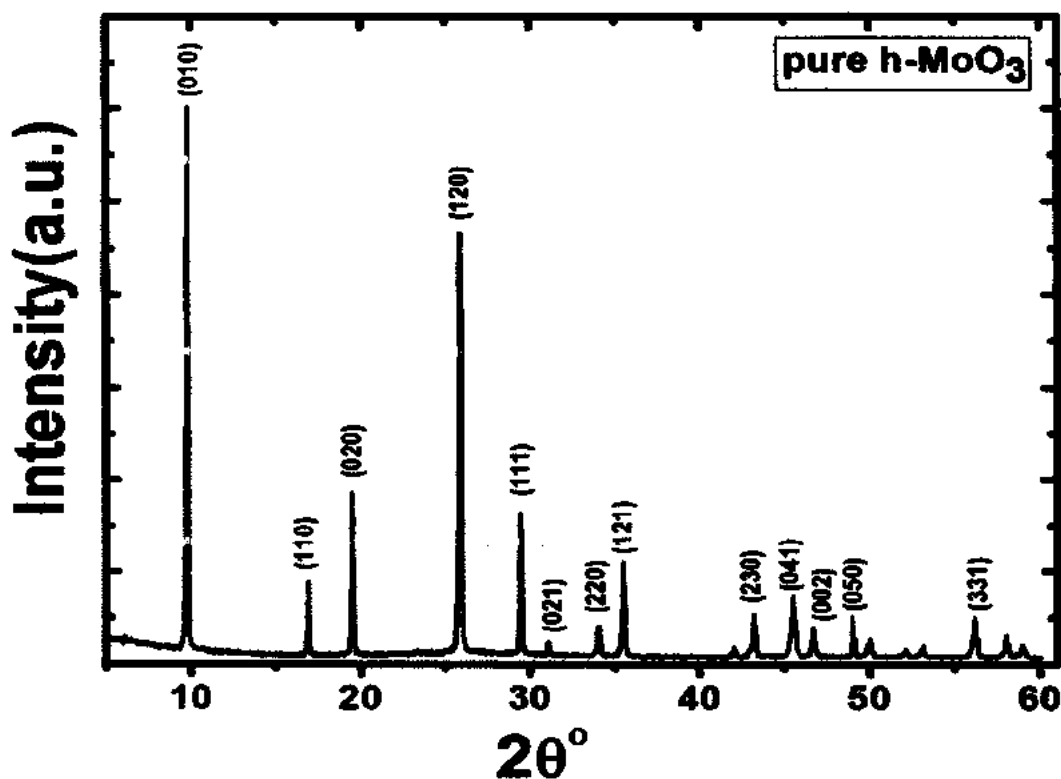


Figure 4.1: The typical XRD pattern of the pure h-MoO₃

The Chromium doped MoO₃ samples were also characterized with the help of XRD, and the apparent XRD spectra of doped samples were compared with pure h-MoO₃ spectra. There is a change in the diffraction peaks of Cr doped samples which are shifted towards right angle. The shift occurs due to Chromium doping, because the ionic radii of the Chromium atom is smaller than that of the Molybdenum atom. So, according to Brag's law when the value of inter atomic spacing "d" decrease then diffraction angle will increase and vice versa, as a result the crystallite size of the particle increases. The XRD spectra of the pure and Cr doped MoO₃ are in hexagonal phase. Diffraction peaks for chromium (Cr) are not observed in the XRD pattern, and all the XRD pattern of doping samples were same. The XRD pattern of the Cr doped MoO₃ as shown in figure 4.2.

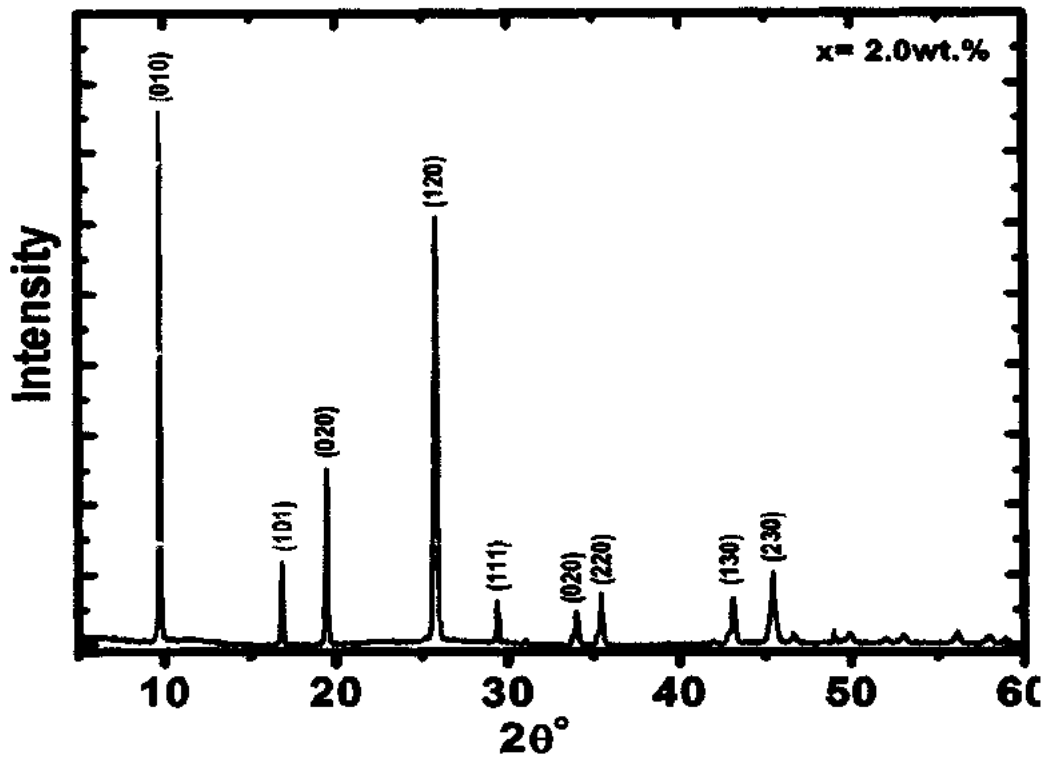


Figure 4.2: XRD pattern of 2wt.% Cr doped MoO₃

4.1.1 Calculation of average crystallite size of MoO₃ particle by using Scherer's formula

To calculate the average crystallite size of the observed curves (XRD pattern) of the samples we used the Scherer's formula, which is already discussed in chapter 3 in detail and is given below [75].

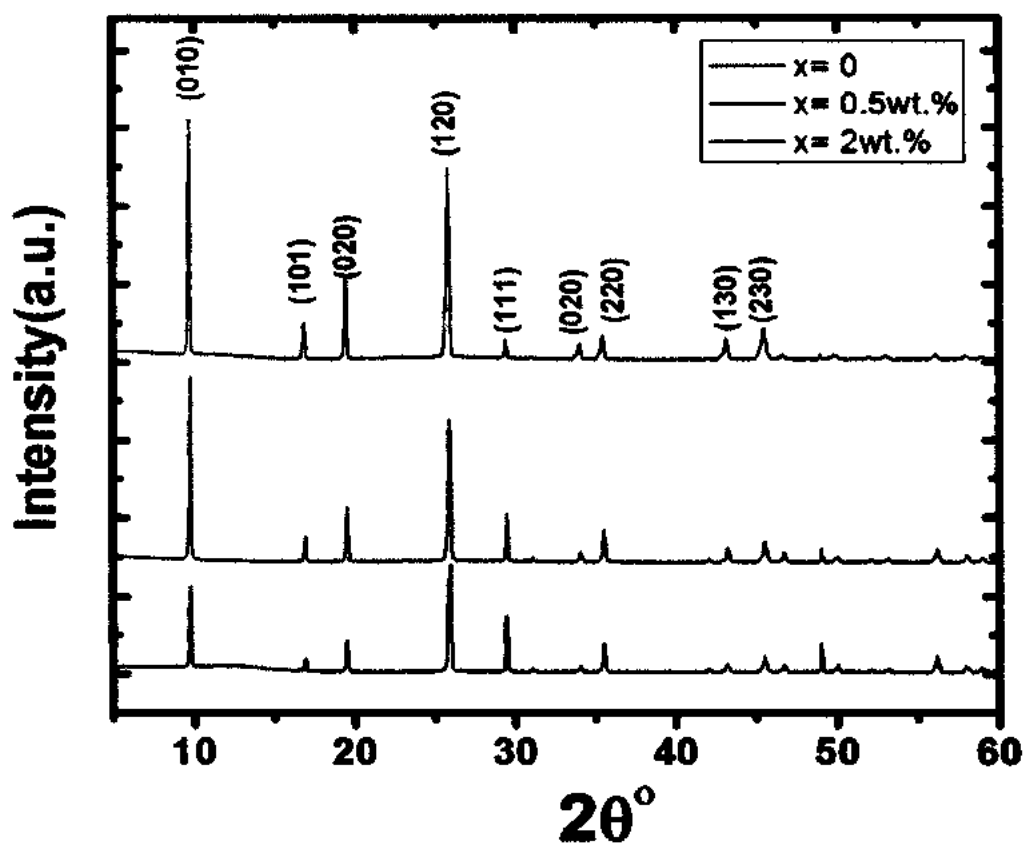
$$D = \frac{k\lambda}{\beta \cos\theta} \quad (4.1)$$

Where λ is the wavelength of the X-ray radiation, k is the shape factor has constant value 0.94, β is the full width at half maxima of the diffracted radiation in radian and θ is the Bragg's angle. Here, in our research work, the crystallite size was calculated by using the high intensity peaks which arised from (010), (020), (120) and (121) planes already mentioned in the XRD pattern as shown in figure 4.1. The average crystallite size of MoO₃ was 38.10995 nm and chromium (Cr) doped MoO₃ is 38.1675 nm which is in good agreement with the reported value, is shown in table 4.1.

Table 4.1: Crystallite size of h-MoO₃

Peak position (2θ)	β (FWHM)	Intensity	Size of single peak (nm)
9.7999	0.0984	100	8.4
19.5280	0.0984	30.11	8.55
25.8698	0.1378	72.58	61.8698
35.5108	0.1181	16.92	73.8

All the synthesized samples are characterized with the help of XRD and no extra impurities peaks were observed of other polymorphous and compared with standard. All the XRD spectra are of pure MoO₃ and Chromium doped MoO₃ are same. The XRD spectra of pure and doped samples are shown in figure 4.3.

Figure 4.3: Combined XRD spectra of pure and doped MoO₃

4.2 Scanning electron microscopy of pure h-MoO₃ and doped CrMoO₃ at different temperature.

Scanning electron microscope (SEM) was employed to study the surface morphology, size and shape of the particles. SEM images give information about growth mechanism and can explain the shape and size of the particles. The SEM image of pure h-MoO₃ sample synthesized at room temperature as shown in the figure 4.4.

4.2.1 SEM of pure h-MoO₃

Figure 4.4 is the SEM image of the synthesized pure h-MoO₃ at low temperature,

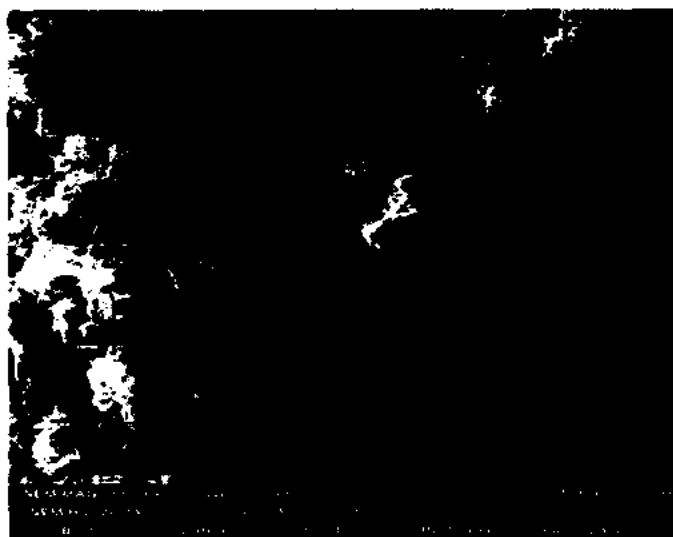


Figure 4.4: SEM image of pure h-MoO₃ at low temperature

In this figure the particles are widely dispersed and are found in combined form. Their size is in micron range and stuck to each other, look like a bunch of nanorods [86]. Therefore size of single nanorods cannot be estimated easily. The size of the nanorod depends on concentration, temperature, chemical reaction and on reaction time. At low temperature size does not reduces and here in my research work the formation of rods are unsuccessful by using this method. The low temperature treatment led the formation of nanoparticles in large size; most of them are defectively synthesized as well as in irregular shape [87]. With these growth conditions we observed strong agglomeration which leads to clusters of the particles. Furthermore some secondary types of structures were also observed. Even after several attempts of the purification we were unable to get rid of these secondary structures. Therefore we decided to change the

experimental conditions for the reaction. In the following figure 4.5 and 4.6 it is discussed that how the reaction temperature leads to change the structure/morphology.

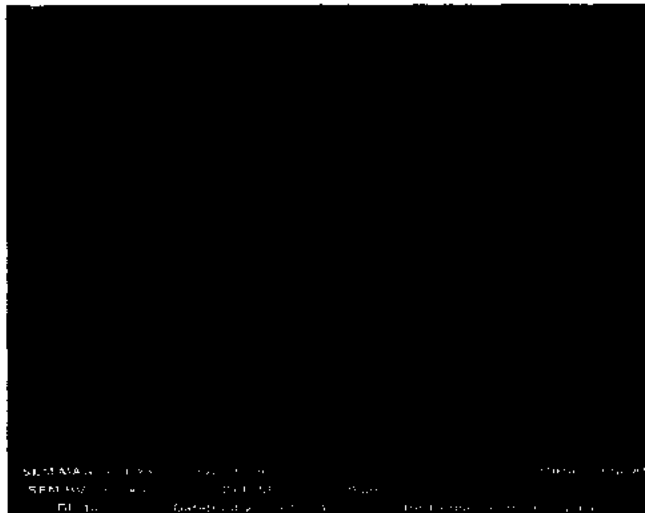


Figure 4.5: SEM image of pure h-MoO₃ at 100° C.

Figure 4.5 is the SEM image of pure MoO₃. The sample is synthesized at 100° C which is the reaction temperature and also changes the mixing temperature from 25 to 35° C, maintaining the pH value same as in previous case. In figure 4.5 it is mentioned that the size of the rods reduce to nano meter range by increasing the temperature. However the structures are not entirely pure. To achieve the purity of the structures, we further increased the reaction temperature. Relatively the pure sample of h-MoO₃ is also achieved at high temperatures, in which the reaction and mixing temperature increased from 100° C to 145° C and 35° C to 40° C, respectively. The pure h-MoO₃ synthesized at 145° C are shown in figure 4.6.

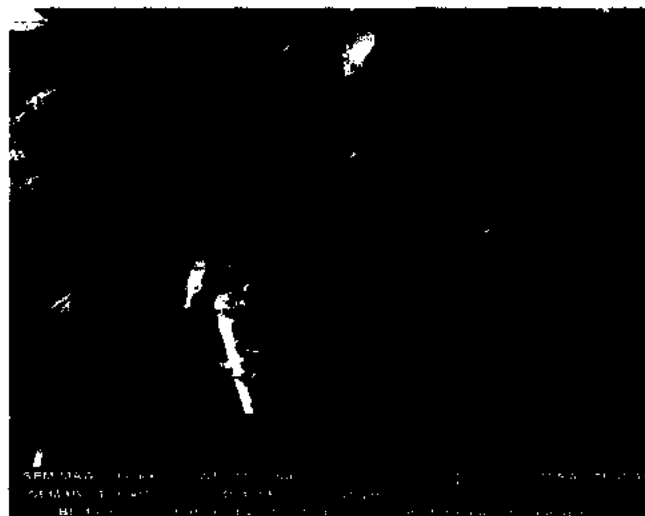


Figure 4.6: SEM image of pure h-MoO₃ at 145° C.

Figure 4.6 is the SEM image of pure h-MoO_3 in powder form, in which the sample is prepared at 145°C and also increased the mixing temperature from 25° to 40°C . The surfaces of the synthesized rods are not uniform however the secondary phases are marginally removed. The hexagonal shape rods like structures are clearly observed. The sharp features of the SEM images also confirm that the particles are of micron size range and shows that the particles are in the form of one dimensional hexagonal rod [87]. The rods which were grown at 100°C have better structure as compared to other structure which were synthesized relatively at low and high temperature. While comparing with reported structure the synthesized structures in our research work are large in size but have the same phase and shape.

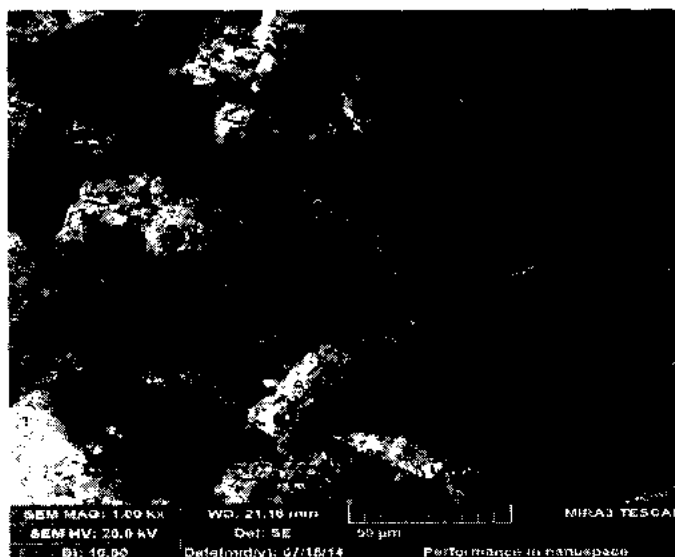


Figure 4.7: SEM image of 2wt. % Cr doped MoO_3

Figure 4.7 is the SEM image of 2 % Chromium doped MoO_3 ; it is not a clear image because the sample was also prepared at low temperature. The Figure contain irregular and rough surface structure nanorods, actually these are the small nanorods which are stuck together in the form of bunch and look like agglomerates which are grown on the surface of nanorods [86]. The rod like structures can be clearly seen as observed in the earlier case without doping. Their size are greater than that of the pure MoO_3 particles Moreover the secondary type of structures are also existing since the sample preparation was carried out at relatively low temperatures.

4.3 Elemental compositional study by (EDX)

The resultant samples were characterized by means of EDX to determine the compositional concentration of the elements present inside the materials. This technique is used

to determine the elemental concentration in the sample. The EDX spectrum of pure h-MoO₃ prepared sample as shown in figure 4.8.

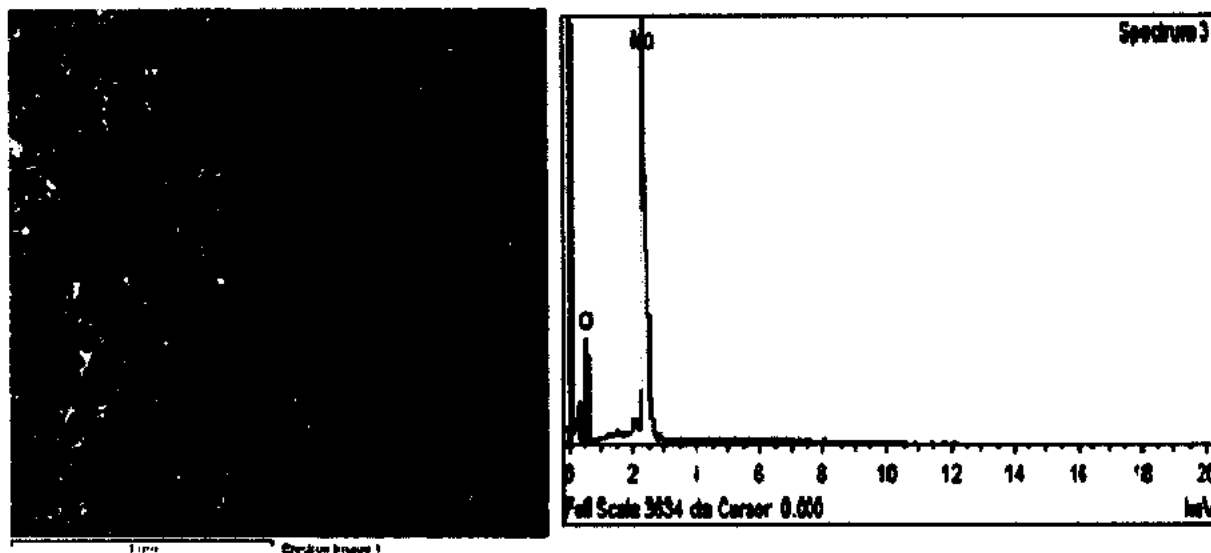


Figure 4.8: EDX spectrum of pure h-MoO₃ at 100^o C.

The given EDX spectrum in the figure 4.8 demonstrated that the synthesized samples only contain Molybdenum (Mo) and Oxygen (O) elements in agreement with the previous reports [36]. These spectra give a good approximation of apparent presence of elements in the sample, compared with theoretical concentration composition [88]. The figure clearly shows the characteristic peaks of molybdenum and oxygen which were well matched with the reported peaks of those elements. It is also observed from the EDX result that the atomic concentration ratio of Mo/O is of about 1/3 confirming the formation of MoO₃ products [89].

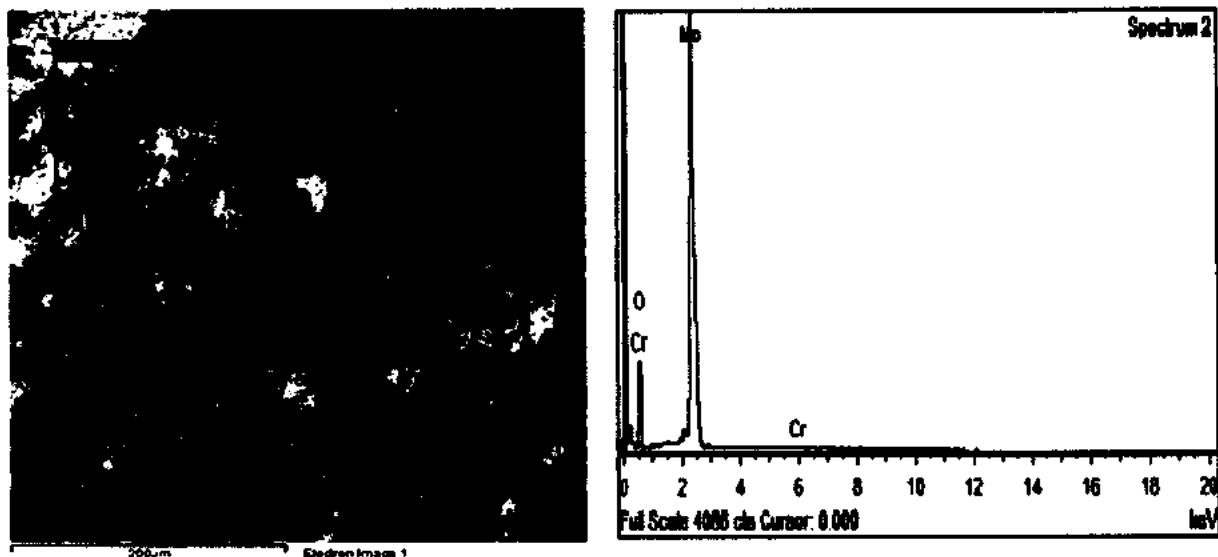


Figure 4.9: EDX spectra of 0.5wt. % Chromium doped h-MoO₃

Figure 4.9 is the EDX spectra of 0.5 % Chromium doped h-MoO₃ which confirm the apparent weight percent of “Cr” element present in the samples is in good agreement with the calculated weight concentration at the time of synthesis in all the particular samples.

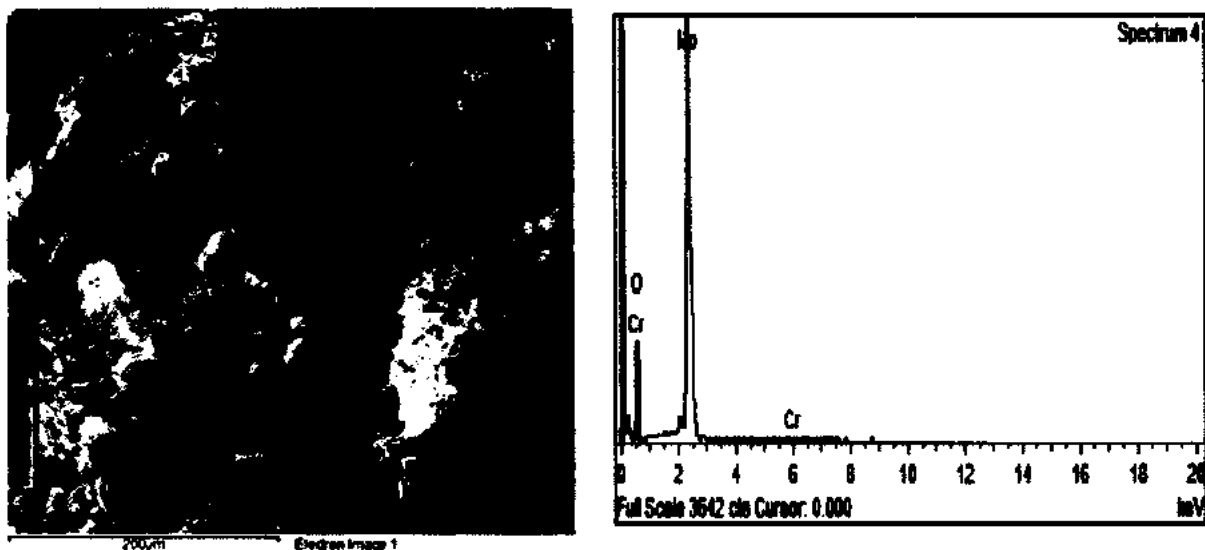


Figure 4.10: EDX spectra of 2wt. % Chromium doped h-MoO₃

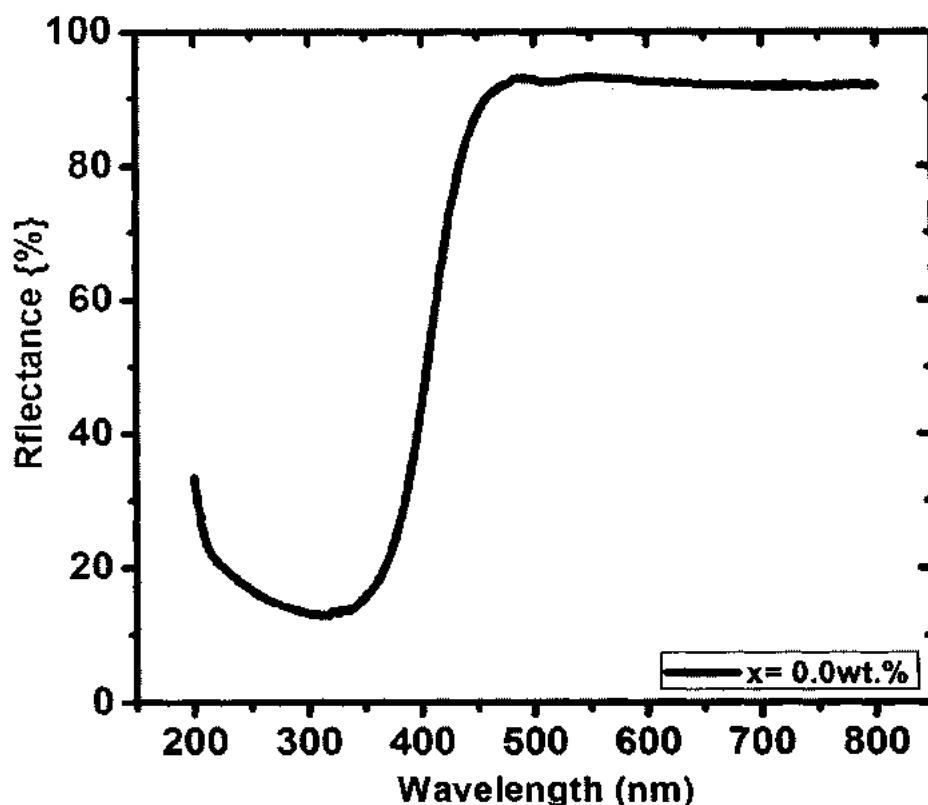
The detail of all the quantitative analysis and compositional study of the entire present element in the material are shown in the table 4.2.

Table 4.2: The Quantitative analysis of pure MoO₃ and Chromium doped MoO₃ samples.

Sample	Mo (wt. %)	O (wt. %)	Cr (wt. %)
Undoped MoO ₃	62.35	37.65	0.00
0.5 % Cr doped MoO ₃	62.72	37.24	0.04
2 % Cr doped MoO ₃	60.64	39.24	0.12

4.4. Optical studies by (DRS)

The optical absorption property of all the synthesized samples of pure MoO₃ and Cr doped MoO₃ are characterized by means of DRS (T-90 UV spectrometer). The DRS spectra of pure h-MoO₃ sample as shown in figure 4.11 [86].

**Figure 4.11:** DRS spectra of pure h-MoO₃

In figure 4.11 the spectra was taken in the range of (200 to 800nm). The maximum reflectance occur between 430 and 800nm to upper absorption, but at 400nm the reflectance decreases due to the elementary absorbance of the material is taken between (valence band to conduction band) [90].

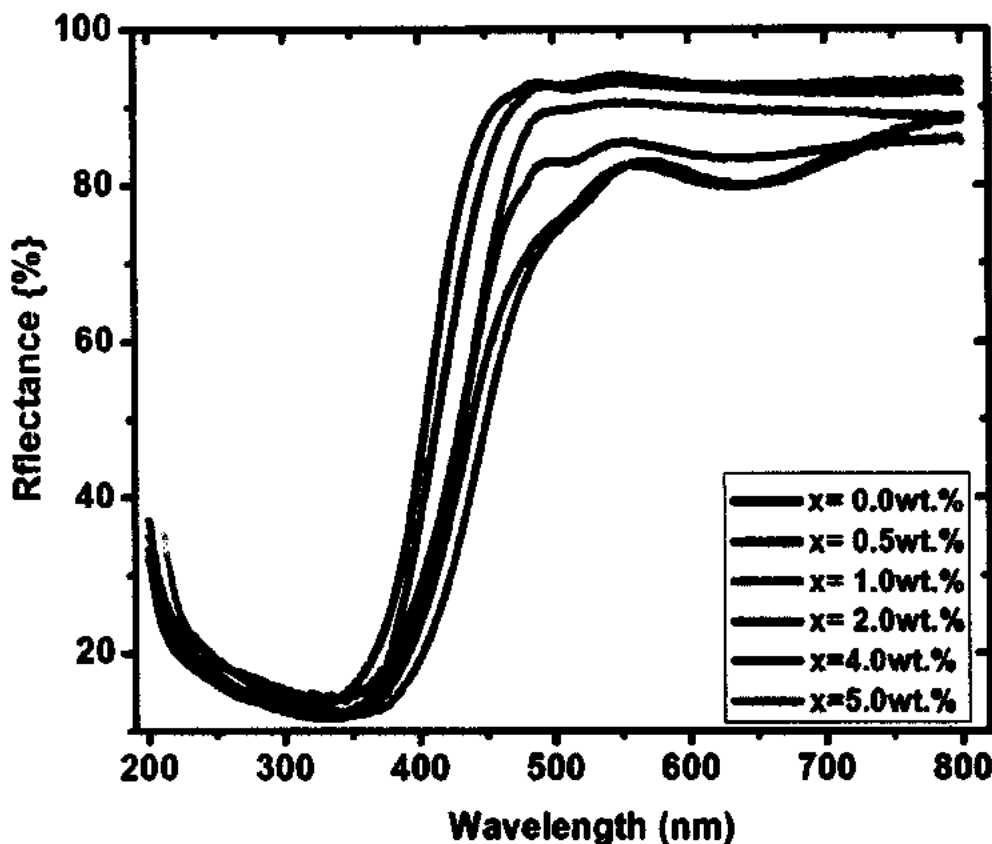


Figure 4.12: Combined DRS spectra of doped and pure MoO₃

Figure 4.12 shows the comparison of the DRS spectra of all samples including doped and pure MoO₃. In the Figure the maximum reflectance occur between 430 and 800nm to upper absorption, but at 400nm the reflectance decreases due to the elementary absorbance of the material is taken between (valence band and conduction band) [90].

In figure 4.12 the DRS spectrum of pure h-MoO₃ and 0.5wt. % Chromium doped MoO₃ exhibit slight difference between them. The absorption of 0.5wt. % doped samples is shifted towards longer wavelength than that of the pure MoO₃. The spectrum of 2wt. % and 4wt. % Chromium doped MoO₃ are also shifted towards larger wavelength and they are same but there is change in the optical band gap. The spectrum shows that the reflectance increases from 390nm and reached to maximum reflectance between 450nm to 800nm for upper absorption. The band gap energy of the samples is calculated by using Kubelka Munk (K-M) function, the K-M graph of all the synthesized samples are shown in figure 4.13 [91].

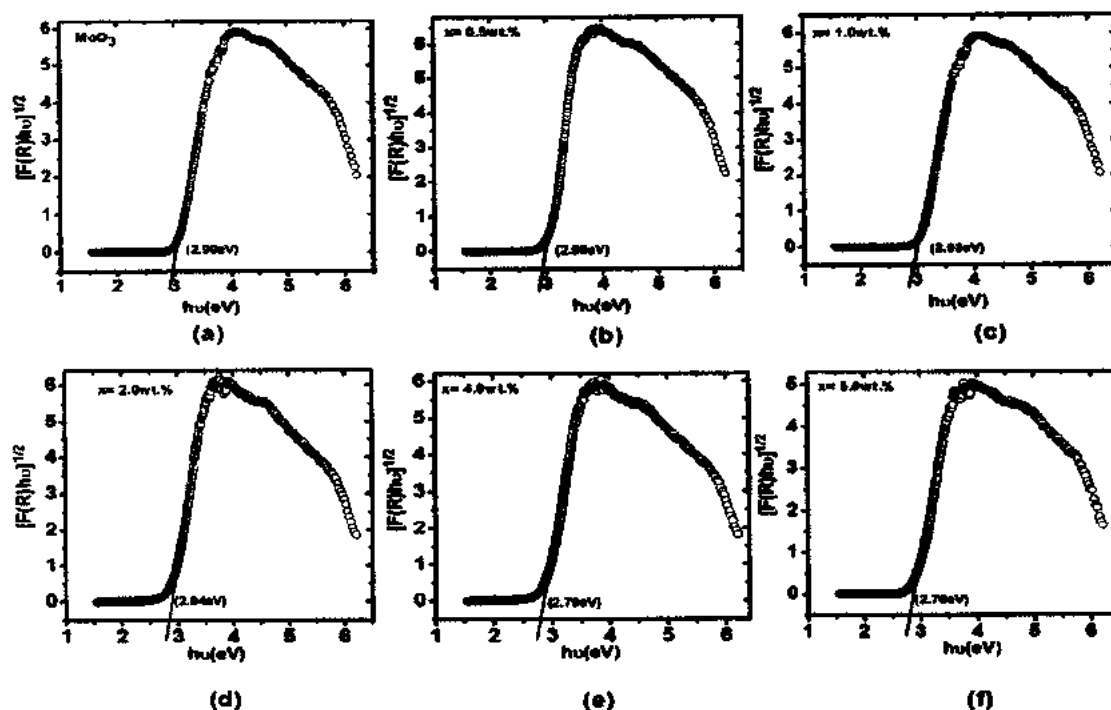


Figure 4.13: Comparison of K-M doped and pure MoO_3 samples

In figure 4.11, the estimated band gap energy of pure h- MoO_3 is 2.99 eV which is greater than that of the Bulk (2.95 eV). The increase in the band gap energy show that the particles size of the synthesise materials was reduced [79]. The band gap energy decreases with doping concentration and also there is possibility due to creation of oxygen vacancy which cause to reduce the band gap of h- MoO_3 . The band gap value of pure and doped samples are shown in the table 4.3.

Table 4.3: Band gap values of doped and pure samples

Doping concentration of Chromium in wt. %	Band gap, eV
Pure h- MoO_3	2.99
0.5 %	2.96
1 %	2.93
2 %	2.84
4 %	2.79
5 %	2.76

For calculating the band gap energy following equation are used [40].

$$F(R_\infty) = (1 - R_\infty)^n \quad (4.2)$$

$$F(R_{\infty}) = \frac{(1-R_{\infty})^2}{2 \times R_{\infty}} = \frac{K(\lambda)}{S(\lambda)} \propto \alpha = \frac{(h\nu - E_g)^n}{h\nu} \quad (4.3)$$

Where $F(R_{\infty})$ is the K-M function, R_{∞} is the diffuse reflectance of infinitely thick sample. $K(\lambda)$ is the absorption coefficient, $S(\lambda)$ is the scattering coefficient, $h\nu$ is the photon energy, E_g is the band gap energy and “n” is integer having the value “2” for direct allowed transition and “1/2” for indirect allowed transition [90]. The graph is plotted between K-M function $F(R_{\infty})$ on the Y-axis where “ $h\nu$ ” is the photon energy is on X-axis, as shown in figure 4.13. In figure 4.13, the estimated band gap energy of pure h-MoO₃ is 2.99 eV which is greater than that of the Bulk (2.95 eV). The calculated band gap values using KM function are plotted as a function of Cr concentration in figure 4.14. The band gap is linearly decreasing with the increasing chromium concentration in MoO₃. The decrease in the band gap was observed up to 7.69% with chromium doping in MoO₃. The overall band gap of the pure MoO₃ is 2.99eV, slightly larger than its bulk value. The increase in the band gap energy show that the particles size of the synthesise materials are in nanometer range [29]. The band gap energy decreases with doping concentration and also there is possibility to create oxygen vacancy which causes to reduce the band gap of metal oxides, because when metal concentration increases in the products then automatically the concentration of oxygen decreases on the surface of the metal oxides. These vacancies may be create due to its re-oxidation or may go to create some defects in the crystal structure [40]. Vanadium element was also reported as a doping element, which was successfully doped in MoO₃ and also tuned their band gap to 2.88eV [41]. The band gap values of pure and doped samples are given in the table 4.3. The band gap energy decreases continuously with doping concentration of Chromium in h-MoO₃ as shown in the figure 4.14.

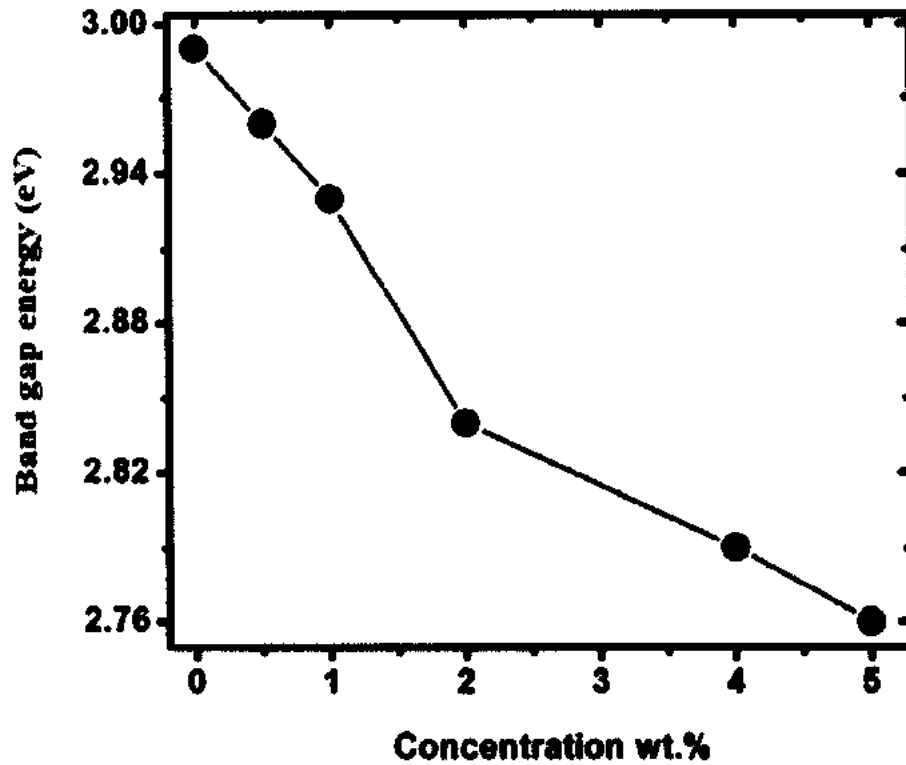


Figure 4.14: Band gap energy versus doping concentration graph.

Figure 4.14 clearly shows that the band gap was decreased to 2.76 eV with 5 % chromium doping, already mentioned in tables 4.3.

Conclusion

In this work, molybdenum trioxide was successfully synthesized in hexagonal phase (h-MoO₃) by solution based chemical co-precipitation method. Crystallinity and hexagonal phase was confirmed by using XRD technique. Scherer's formula was used to calculate the crystallite size of (h-MoO₃), which was in nanometer range. It is confirmed from SEM images that the synthesized rods have one dimensional hexagonal structure. Initially, it was observed that at low temperature the growth of rods are not uniform, but at relatively higher temperatures the structure was regular and reasonable. It is confirmed from EDX results that the products contain only molybdenum and oxygen elements. These spectra give a good approximation of apparent presence of elements in the samples, compared with real concentration of the precursor solution. It is observed from the EDX result that the atomic concentration ratio Mo/O is of about 1/3, confirming the MoO₃ product. The optical study absorption and band gap was studied by means of UV/ visible spectroscopy. The band gap of pure MoO₃ and chromium doped samples was calculated from the optical absorption studies. Moreover, for tuning the optical properties and band gap, Cr was doped in the MoO₃ and its effects were studied systematically. It was observed that the band gap decreases with chromium doping. In this thesis work, the band gap of MoO₃ was decreased from 2.99 eV for pure samples to 2.76 eV with different doping concentration of chromium. From these result, it was observed that the MoO₃ nanorods were synthesized in nanometer range as well as chromium was doped successfully.

In future, we will use it as a p-type material in photovoltaic cell for hole conduction inside the device, in which the nanorods can be grown on some transparent glass substrates to make a hetero-junction with other cathodic materials.

References

- [1]. W. D. Callistar Jr, and D. G. Rethwisch, "Material Science and Engineering" 8th Edition. Department of Metallurgical Engineering the University of Utah (2008).
- [2]. M. A. Wahab, Solid State Physics, "Structure and Properties of materials", 3rd Edition Narosa Publishing Hous, New Delhi and α -Scirnce, Oxford, Uk (2009).
- [3]. M. P. Groover "Fundamentals of Modern Manufacturing 2/e" Jhon Wiley & Sons, Inc. (2002).
- [4]. W. Casri, Nanocomposites of Polymers and metals or Semiconductors: Historical Background and optical properties. *Macromolecular Rapid Communications*, **21**, 705-722 (2000).
- [5]. R. K. Puri and V. K. Babbar. "Solid Stae Physics" S-Chand Series ISO 9001: New Delhi (2000).
- [6]. D. A. Neamen, *Semiconductor Physics and Devices*, McGraw-Hill Education (India). Vol 3rd (2007).
- [7]. M. Shur, *Physics of Semiconductor Devices*. Englane wood Cliffs, NJ: Prentice-Hall, Inc. (1990).
- [8]. K. E. Drexler, *Nanosystems; Molecular Machinery, Manufacturing and Computation*, 1st Edition, John Wiley & Sons Publisher (1992).
- [9]. S. Santosh, S. Sons, J. and Sugandha, *Cutaneous and Aesthetic Surgery* **10**, 32-33 (2010).
- [10]. C. Buyea. I. Pacheco, K. Robbie, *Nanomaterials and Nanoprticles: Sources and Toxicity*, 1st Edition, Jhon Wiley & Sons Publisher (2007).
- [11]. A. R. West. *Basic Solid State Chemistry*, 2nd Edition, Jhon Wiley & Sons Publisher (1997).
- [12]. T. Harper, *J. American Chemical Society*. **81**, 14 (2003).
- [13]. G. C. Bond, C. Louis, D. T. Thompson, *Catalysis by Gold*, Imperial College Press, London, 2006.
- [14]. M. A. Reed, C. Zahou, C. J. Muller, T. P. Burgin, and J. M. Tour, *Nanostructures and Nanomaterials*, 1st Edition, Royal Society and Royal Academy of Engineering Publisher, (1997).

- [15]. J. Baran, and O. Cabrera, Use of Surface-Modified Nanoparticles for Oil Recovery, 1st Edition, US Publisher, (2003).
- [16]. R. Seigel, and W. Hu, Roco, Nanostructure Science and Technology, 1st Edition. kluwer Academic Publisher, (1999).
- [17]. M. Roco, C. William, and R. S. Alivisatos, Nanotechnology Research Directions, 3rd Edition, kluwer Academic Publisher (2000).
- [18]. S. S. Mahajan, S. H. Mujawar, P. S. Shinde, A. I. Inamdar and P. S. Patil, Int. J. Electrochem. Sci 3, 953 (2008).
- [19]. J. L. G. Fierro, Metal Oxides: Chemistry and Applications, CRC Press Florida (2006).
- [20]. V. E. Henrich, and P. A. Cox, The Surface Chemistry of Metal Oxides, Cambridge University Press, Cambridge, UK, (1994).
- [21]. C. Noguera, Physics and Chemistry at Oxide Surfaces, Cambridge University Press, Cambridge, UK (1996).
- [22]. A. R. Jose, and F. G. Marcos, Synthesis, Properties, and Applications of Oxide Nanomaterials, Willey, New Jersey (2007).
- [23]. N. Greenwood, and A. Earnshaw, Chemistry of the Elements, 2nd Edition, Oxford: Butterworth- Heinemann Publisher (1997).
- [24]. K. Bandyopandhyay, J. Mater. Sci. 21, 16 (1981).
- [25]. G. Ertl, H. Knozinger, and J. Weitkamp, Handbook of Heterogeneous Catalysis, Wiley-VHC, Weinheim (1997).
- [26]. J. P. Jolivet, Metal Oxide Chemistry and Synthesis: From Solution to Solid State, Wiley, Chichester (2000).
- [27]. G. R. Patzke, F. Krumeich, and R. Nesper, Oxidic nanotubes and nanorods - Anisotropic modules for a future nanotechnology, Angew. Chem. Int. Ed. 41, 2446-2461 (2002).
- [28]. Y. Y. Wu, H. Q. Yan, M. Huang, B. Messer, J. H. Song, and P. D. Yang, Inorganic semiconductor nanowires: Rational growth, assembly, and novel properties, Chem. Eur. J. 8, 1261-11268 (2002).
- [29]. C. N. R. Rao, F. L. Deepak, G. Gundiah, and A. Govindaraj, Inorganic nanowires, Prog. Solid State Chem. 31, 5-147 (2003).
- [30]. Z. R. Dai, Z. W. Pan, and Z. L. Wang, Novel nanostructures of functional oxides synthesized by thermal evaporation, Adv. Func. Mater. 13, 9-24 (2003).

- [31]. D. V. London J. M. Friedrich, and F. C. Walsh, Protonated titanates and TiO₂ nanostructured materials: Synthesis, properties, and applications, *Adv. Mater.* **18**, 2807-2824 (2006).
- [32]. G. C. Bond, C. Louis, and D. T. Thompson, *Catalysis by Gold*, Imperial College Press, London (2006)
- [33]. P. Fratzl, Biomimetic materials research, *Journal of the Royal Society Interface* **4**, 637-42 (2007).
- [34]. V. E. Henrich, and P. A. Cox, *The Surface Science of Metal Oxides*, Cambridge University Press, Boston (1994).
- [35]. C. Lang, D. Schuler, and D. Faivre, Synthesis of magnetite nanoparticles for bio-and nanotechnology: genetic engineering and biomimetics of bacterial magnetosomes. *Macromolecular Biosciences* **7**, 144-51(2007).
- [36]. S. S. Mahajan, S. H. Mujawar, P. S. Shinde, A. I. Inamdar and P. S. Patil, Concentration Dependent Structural, Optical and Electrochromic Properties of MoO₃ Thin Films, *Int. J. Electrochem. Sci* **3**, 953-960 (2008).
- [37]. L.A. Bursill, *Proc. R. Soc. London A* **311**, 27 (1969).
- [38]. L.A. Bursill, *Acta. Crystallogr. Sect. A* **28**, 187 (1972).
- [39]. C. Bouchy, C. Pham-Huu, B. Heinrich, C. Chaumont, and M. J. Ledoux *J. Catalysis* **190**, 92-103 (2000).
- [40]. L. A. Kihlberg, Refinement of the crystal structure of Molybdenum trioxide, *Ark. Kemi* **21**, 471 (1963).
- [41]. M.C. Rao, K. Ravindranadh, A. Kasturi, and M. S. Shekhawat *Res.J. Recent Sci* **2(4)**, 67-73 (2013).
- [42]. S. A. Tomas, M. A. Arvizu, O. Zelaya-Angel and P. Rodriguez, Effect of ZnSe doping on the photochromic and thermochromic properties of MoO₃ thin films, *J. Thin Solid Films* **518**, 1332-1336 (2009).
- [43]. I. Esmat, and A. Saad, Dielectric properties of molybdenum oxide thin films, *J. Optoelectro. Adv. Matt* **7**, 2743-2752 (2005).
- [44]. L. Lim, M. Guan, G. Cao, Y. Li, and Y. Zeng, Low operating voltage and high power efficiency OLED employing MoO₃-doped CuPc as hole injection layer, *Displays* **33**, 17-20 (2012).

- [45]. E. Comini, L. Yubao, Y. Brando and G. Sberveglieri, Gas sensing properties of MoO₃ nanorods to CO and CH₃OH, *J. Chem. Phys. Lett.* **407**, 368-371 (2005).
- [46]. V. Shrotriya, G. Li, Y. Yao, C. W. Chu and Y. Yang, Transition metal oxides as the buffer layer for polymer photovoltaic cells, *J. Appl. Phys. Lett.* **88**, (1-6) (2006).
- [47]. L. Arunkumar, H. Vijayanand, S. Basavaraja, and A. Venkataraman, Synthesis of MoO₃ and its polyvinyl alcohol nanostructured film, *Bull. Mater. Sci.* **28**, 477-481 (2005).
- [48]. C. S. Hsu, C. C. Chan, H. T. Huang, C. H. Peng and W. C. Hsu, Electrochromic properties of nanocrystalline MoO₃ thin films, *J. Thin Solid Films.* **516**, 4839-4844 (2008).
- [49]. G. Binnig and H. Rohrer, *IBM J. Res. Dev.* **30**, 355 (1986).
- [50]. M. Tsukada, K. Kobayashi, N. Isshiki and H. Kageshima, *Surf. Sci. Rep.* **13**, 265 (1991).
- [51]. T. R. Albrecht, and C. F. Quate, *J. Vac. Sci. Technol. A.* **6**, 271 (1988).
- [52]. Y. Zhao, J. Liu, Y. Zhou, Z. Zhang, Y. Xu, H. Naramoto and S. Yamamoto *J. Phys.: Condens. Matter.* **15**, L547-L552 (2003)
- [53]. C. J. Brinker, and G. W. Scherer. *Sol - gel science: The Physics and the chemistry of sol gel processing*, Academic Press, Inc. London (1990).
- [54]. L. L. Hench, *J. K. West. Chem. Rev.* **33**, 90 (1990).
- [55]. L. J. Fu, H. Liu, C. Li, Y. P. Wu, E. Rahm, R. Holze, and H. Q. Wu, *Prog. Mater. Sci.* **50**, 881-928 (2005).
- [56]. H. Liu, Y. P. Wu, E. Rahm, R. Holze, and H. Q. Wu. *J. Solid State Electrochem.* **8**, 450-466 (2004).
- [57]. L. Predoana, A. Barau, M. Zaharescu, H. Vassilchina, N. Velinova, B. Banov, and A. Mornchilov, *J. European Cera. Soc.* **27**, 1137-1142 (2007).
- [58]. Q. Chena, J. Wang, Z. Tang, W. Hea, H. Shao, and J. Zhang, *Electrochim. Acta.*, **52**, 2551-2557 (2007).
- [59]. D. H. Chen, and X. R. He, *Mater. Res. Bull.* **36**, 1369-1377 (2001).
- [60]. B. J. Hwang, R. Santhanam, and D. G. Liu, *J. Power Sources* **97**, 443-446 (2001).
- [61]. Y. D. Zhong, X. B. Zhao, G. S. Cao, J. P. Tu, and T. J. Zhu, *J. Alloys Compd.* **420**, 298-305 (2006).
- [62]. J. T. Son, and H. G. amanic, *J. Power Sources* **147**, 220-226 (2005).
- [63]. Y. Zhang, H. Cao, J. Zhang, and B. Xia, *Solid State Ionics* **177**, 3303-3307 (2006).

- [64]. T. H. Cho, Y. Shiosaki, and H. Noguchi, *J. Power Sources* **159**, 1322-1327 (2006).
- [65]. M. J. Godinho, R. F. Goncalves, L. P. S. Santos, J. A. Varela, E. Longo, and E. R. Leite, *Mater. Lett* **61**, 1904-1907 (2007).
- [66]. Y. Zhang, H. Cao, J. Zhang, B. Xia, *Solid State Ionics*. **177**, 3303-3307 (2006).
- [67]. B. Gaikwad, S. C. Navale, V. Samuel, A. V. Murugan, and V. Ravi, *Mater. Res. Bull* **41**, 347-353 (2006).
- [68]. V. Nirupama, M. C. Sekhar, T. K. Subramanyam and S. Uthanna, Structural and electrical characterization of magnetron sputtered MoO₃ thin films, *J. Phys. Conf. Ser* **208**, 12101-12106 (2010).
- [69] G. Xu, X. Zhang, W. He, H. Liu, H. Li, and R. I. Boughton, *Materials Letters* **60**, 962-965 (2003).
- [70]. B. D. Cullity, S. R. Stock, S. Stock, *Elements of X-Ray Diffraction*, 3rd Edition, Prentice, Ha **11**, 163-168 (2001).
- [71]. P. Misra, and M. Dubinskii. "Ultraviolet Spectroscopy and UV Lasers" Taylor and francis **7**, 16-17 (2002).
- [72]. H. P. Klug, and L. E. Alexander, *X-ray Diffraction Procedures for Polycrystalline and Amorphous Materials*, Wiley, New York, (1954).
- [73]. S. H. Lee, M. J. Seong, C. Edwin Tracy, A. Mascarenhas, J. Roland Pitts, and K. Satyen Deb. *Raman spectroscopic Vol. 2(4)*, 67-73 (2013)
- [74]. X. D Chen, C. C. Ling, S. Fung, C. D. Beling, Y. F. Mei, and R. K. Y. Fu, "Current transport studies of ZnO/p-Si heterostructures grown by plasma immersion ion implantation and deposition". *Appl. Phys. Lett.* **88**, 132-104 (2006).
- [75]. H. G. Jlang, M. Ruhle, and E. J. Lavernia, *J. Mater. Res* **14**, 549-559 (1999).
- [76]. M. T. Weller, *Inorganic Materials Chemistry (Oxford Chemistry Primers)*, Oxford University Press, UK (2001).
- [77]. G. R., Adair, J. H. and R. E. Newnham, *J. Mater. Sci* **25**, 34-36 (1990).
- [78]. S. Wischnitzer. *Introduction to Electron Microscopy*, Pergamon Press (1998).
- [79]. R. W. Cahn, P. H. Haasen, and E. J. Kramer, VCH Germany, 2A (1992).
- [80]. M. Willander, K. Ul Hasan, O. Nur, A. Zainelabdin, and S. Zaman, G. Amin. "Recent progress on growth and device development of ZnO and CuO nanostructures and graphene nanosheets". *J.Mater. Chem.* **22**, 2337-2350 (2012).

- [81]. C. R. Brundle, and C. A. Evans, Encyclopedia of Materials Characterization, Butterworth-Heinemann, Boston (1992).
- [82]. G. Goldstein, I. Nebury, D. E. Echlin, P. Joy, and D. C. Eifshin, Scanning Electron Microscopy and X-ray microanalysis, 2nd Edition, Plenum Press Publisher (1981).
- [83]. Y. R. Sharma, Elementry Organic Spectroscopy. 1st Edition. S. Chand Publisher (2010).
- [84]. G. R. Chatwal, Instrumental Methods of chemical analysis. 1st Edition. Himalaya Publisher (2010).
- [85]. A. Chithambararaj, and N. S. Sanjini, "Flower-like hierarchical h-MoO₃: new findings of efficient visible light driven nano photocatalyst for methylene blue degradation." Catalysis Science & Technology **3**, 11405-1414 (2013).
- [86]. A. C. Angamuthuraj, and Chithambararaj *et al.* Beilstein J. Nanotechnol **2**, 585-592 (2011).
- [87]. V. V. Atuchin, T. A. Gavrilova, V. G. Kostrovsky, L. D. Pokrovsky, and I. B. Troitskaia, J. neorganichskre Materialy **44**, 714-719 (2008).
- [88]. N. R. Dighore, S. P. Jadav, S. T. Gaikwad, and A. S. Rajbhaj, J. Engineering Research and Applications **6**, 135-139 (2014).
- [89]. L. Chibane, M. S. Belkaid, and M. Pasquinell, . ICREPQ (2012).
- [90]. T. He, and J. Yao. J. Photochem. Photobiol., C **4**, 125-143 (2003).
- [91]. J. Liu, Y. Lu, J. Liu, X. Yang, and X. Yu, J. Alloys Compd. **496**, 261-264 (2010).
- [92]. Y. Mao, W. Li, and X. Sun, Cryst. Eng. Comm. **14**, 1419 (2012).